Wetland & Lake monitoring—Case study Poyang Lake & Erhai Lake

Liqiong Chen & Xiaoling Chen

ESA–MOST China Dragon 4 Cooperation

2019 ADVANCED INTERNATIONAL TRAINING COURSE IN LAND REMOTE SENSING

中欧科技合作“龙计划”第四期 2019年陆地遥感高级培训班

18 to 23 November 2019 | Chongqing University, P.R. China

培训时间:2019年11月18日-23日 主办方:重庆大学

Wetland & Lake monitoring—Case study Poyang Lake

Liqiong Chen & Xiaoling Chen

State key Laboratory of Information Engineering in Surveying, Mapping and Remote sensing (LIESMARS), Wuhan University

Introduction: How wetland connects lake and land?

Basic Principles

Applications

- Water body
- Wetland
- Eutrophication

Introduction

Global change leads global challenge

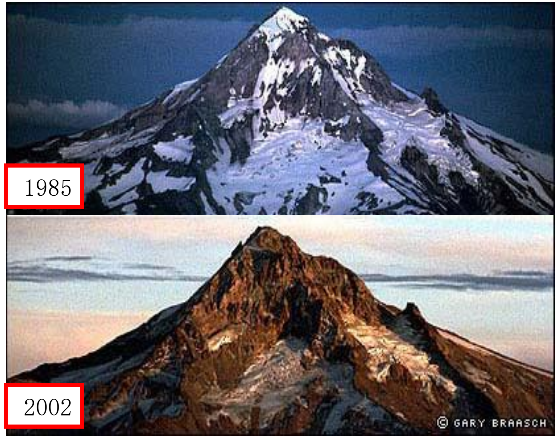

Ice is melting

Islands are disappearing

Lakes Water Change in China Since 30 Ka BP

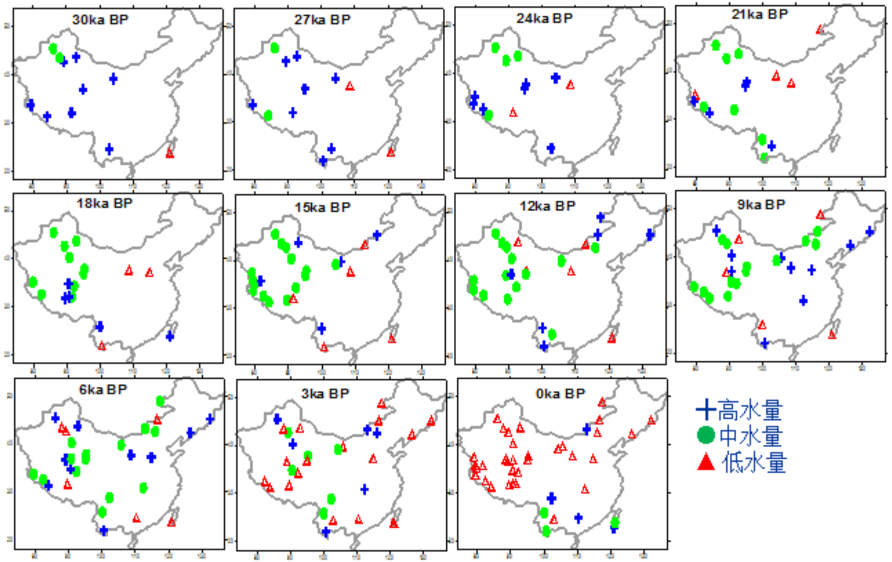

Xue B,et.al.,2003，Science China

Dynamic process of Dongting Lake

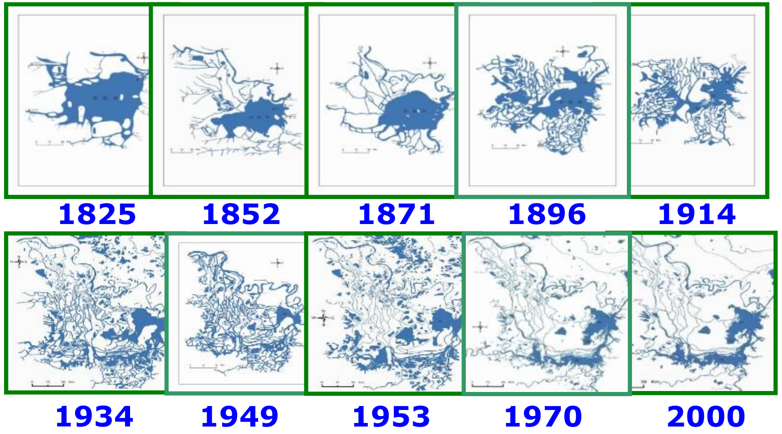

Only three river-connected lakes are in Yangtze river

The vegetation of most of the lakes in Yangtze plain showed a decreased trend

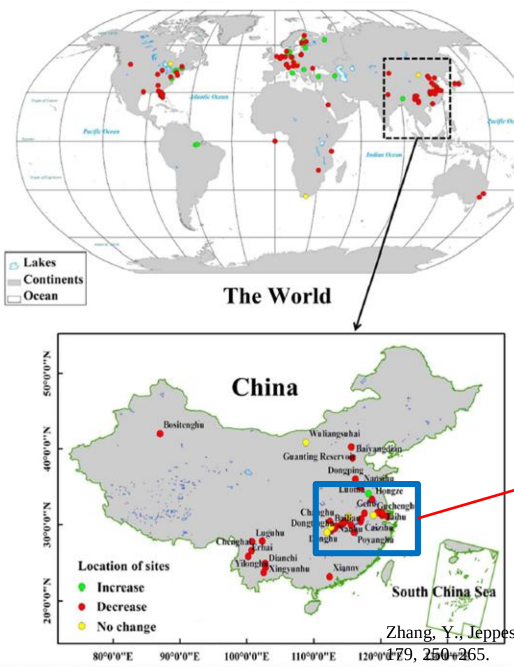

Fig. 1. Spatial distribution of study sites around the world and in China. Green indicates a decrease, red an increase, and yellow no change in aquatic vegetation. (For interpretation of the references to color in this figure legend, the reader is referred to the web version of this article.)

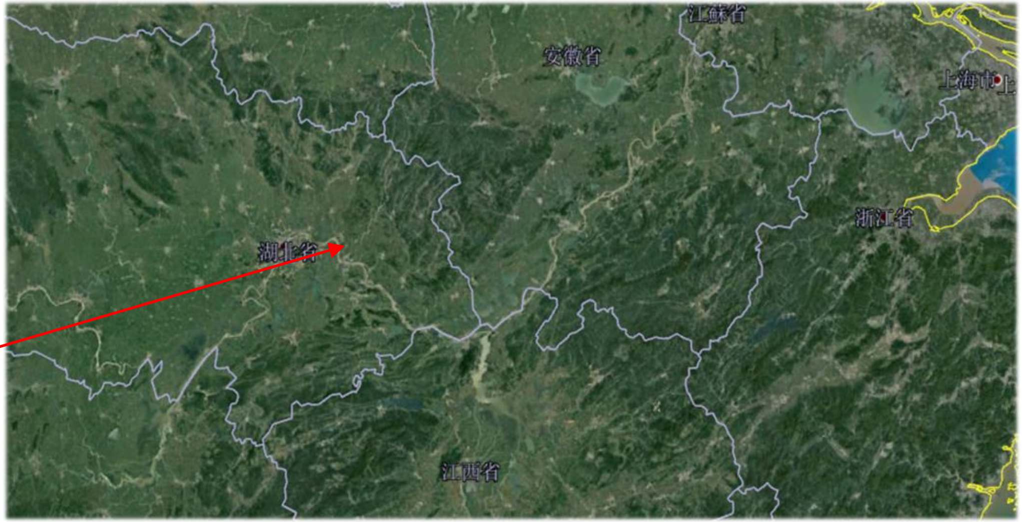

Zhang, Y., Jeppesen, E., Liu, X., Qin, B., Shi, K., Zhou, Y., Thomaz, S.M., Deng, J., 2017.global loss of aquatic vegetation in lakes. Earth Sci. Rev. 179, 250-265.

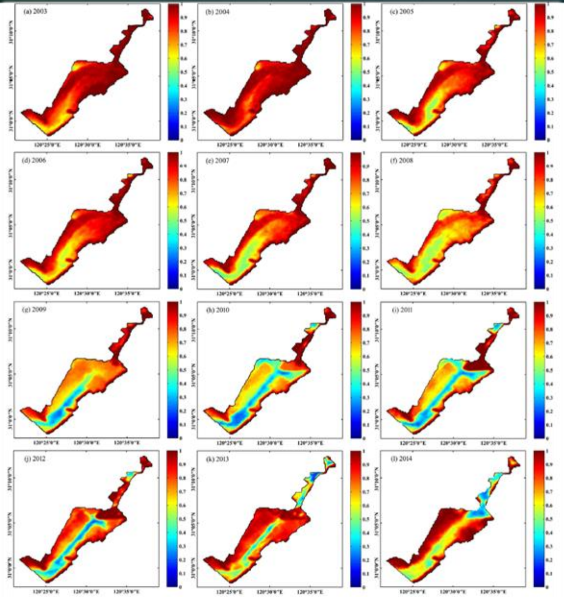

Figure 3. MODIS-Aqua-derived yearly climatology VPF from 2003 to 2014. 2003 (a), 2004 (b), 2005 (c), 2006 (d), 2007 (e), 2008 (f), 2009 (g), 2010 (h), 2011 (i), 2012 (j), 2013 (k), and 2014 (l).

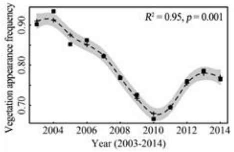

Figure 4. Long-term trends in the VPF from 2003 to 2014 in Eastern Lake Taihu. The dash line indicates fitted values of VPF data versus year by GAM.

Taihu Lake

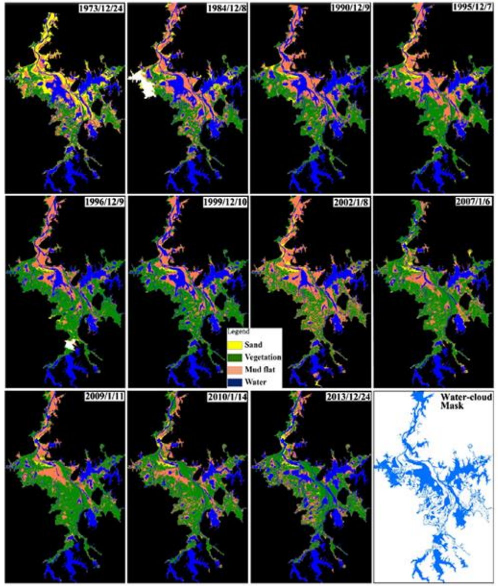

Fig. 6. Classification maps of Poyang Lake from four decades of Landsat observations between 1973 and 2013. The last panel shows the maximum inundation and cloud mask for further area statistics.

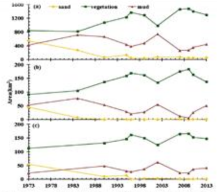

Poyang Lake

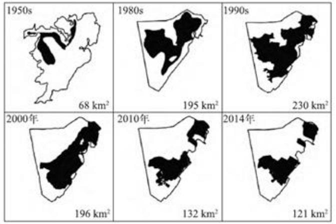

图 3 微齿眼子菜群落 1950s—2014 年分布范围及面积变化

Fig.3 The distribution and area of *Potamogeton maackianus* community from 1950s to 2014

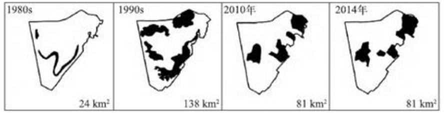

图 4 金鱼藻群落 1980s—2014 年分布范围及面积变化

Fig.4 The distribution and area of *Ceratophyllum demersum* community from 1980s to 2014

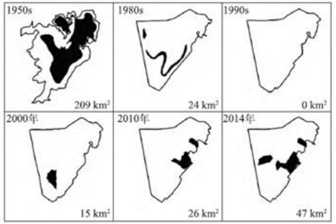

图 5 轮叶黑藻群落 1950s—2014 年分布范围及面积变化

Honghu Lake

Challenges

- Water Quality
- Wetland Ecology
- Public Health

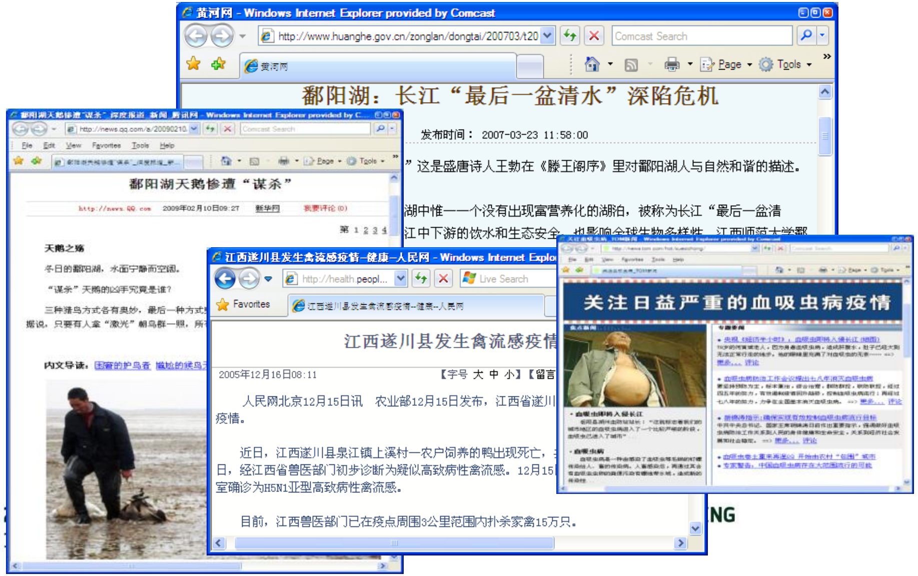

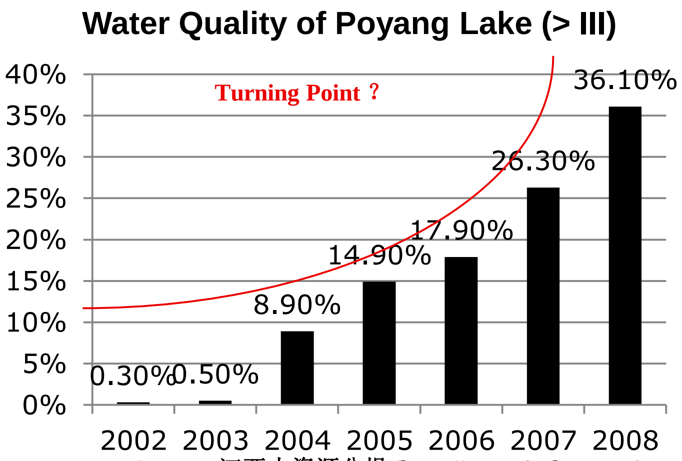

Source: 江西水资源公报 (http://www.jxsl.gov.cn/)

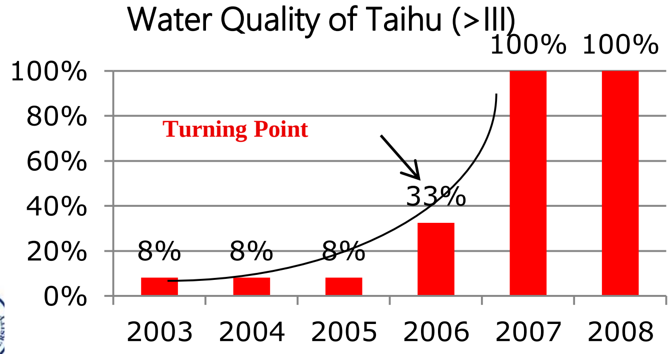

Source:太湖流域及东南诸河水资源公报

感高级培训班
主办方：重庆大学

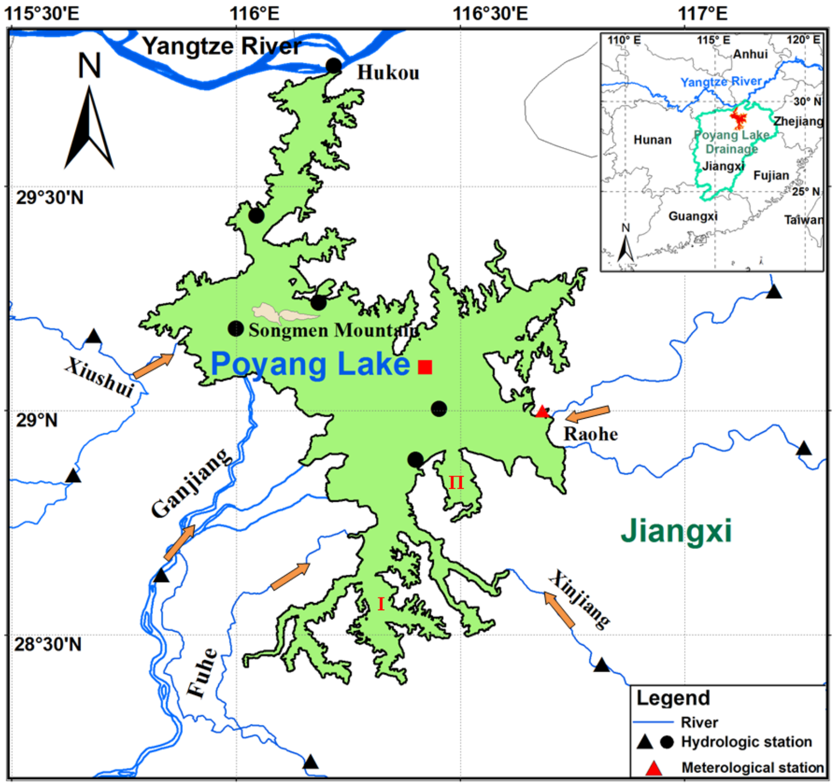

❖ Largest freshwater lake in China

✓Inundation: >3000km²(wet season)

✓Drainage: 162,200 km²

❖ Water flow from south to north, and discharge into the Yangtze River

❖ Water income: precipitation, local rivers and Yangtze River (reversal flow)

❖ Highly water dynamics & world famous wetlands

✓ Migratory bird

✓ Schistosomiasis

❖ Lagged economic development

Poyang Lake is one of the most frequently flooded and drought areas in China. Rapid changes of the inundation area play an important role in affecting the wetland ecosystem as the habitat for migrating birds

Basic Principles

Integration of Space-born and Ground Observation for Dynamic Monitoring

Wetland
Dynamics:
Pattern,
Boundary uncertainty

Lake
Dynamics :
Area,
Bottom ,
Water Quality,
Water Quantity…

Watershed
Surface Process:
LUCC,
Soil erosion,
Non-point source pollution

Hydro-Ecological Modeling

Spatial Information Sharing System

Mission capability

Algorithms

In-situ observations

Operational capability

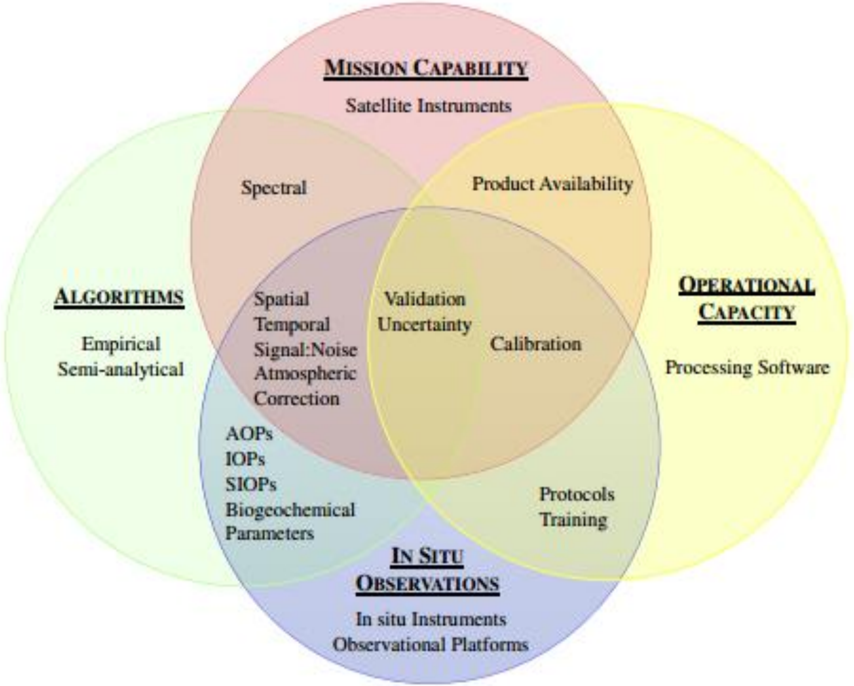

Colleen B. Mouw，2015, Aquatic color radiometry remote sensing of coastal and inland waters: Challenges and recommendations for future satellite missions, Remote sensing and environment

How to choose sensors for you study areas?

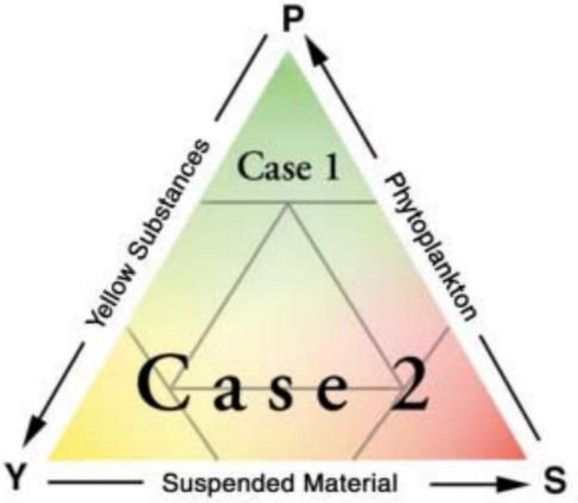

Small area

Complexity color

Dynamic changes

Spatial resolution

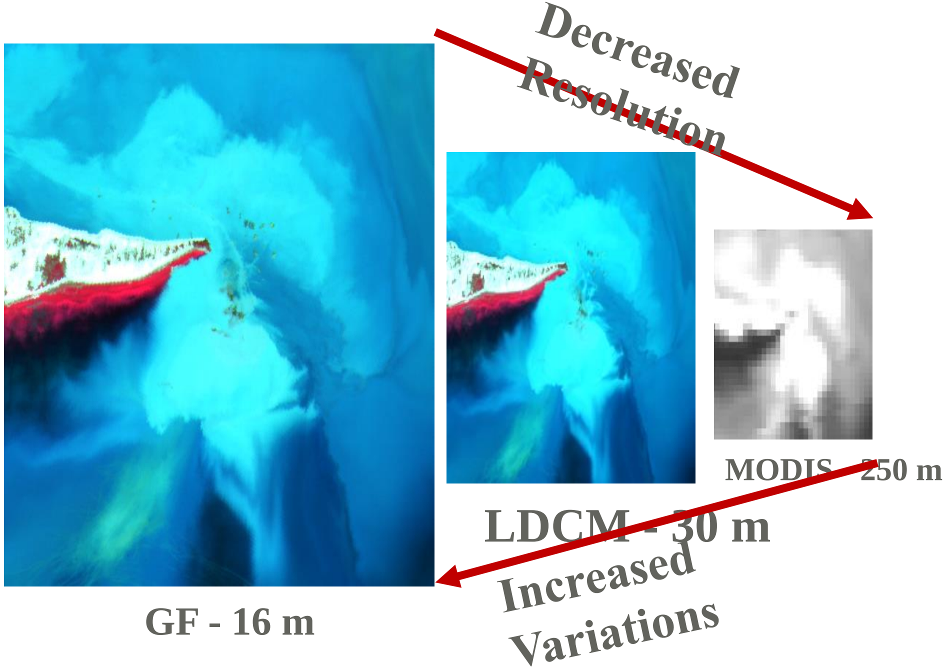

Sentinel-2A MSI, Dec. 31,2016
RGB:432, 30M

Sentinel-3 OLCI, Dec. 05,2016
RGB:864, 300M

Radiative resolution

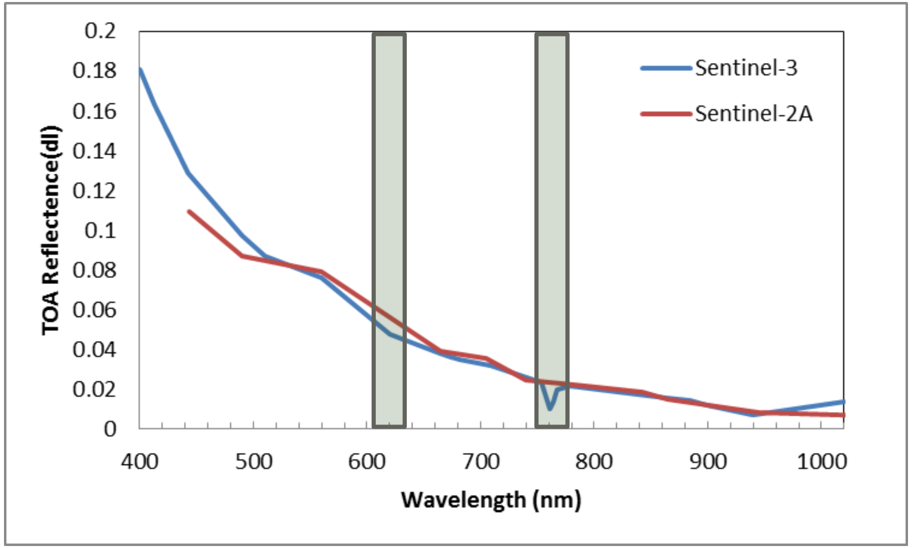

OLCI	Function
400nm	Aerosol correction, improved retrieval
412.5nm	Yellow substance(turbidity)
442.5nm	Chl absorption max
490nm	High Chl, other pigments
510nm	CHL, sediment, turbidity, red tide
560nm	Chl absorption min
620nm	Sediment
665nm	Chl(2nd Chl abs. max), sediment, yellow substance
673.35nm	Improved fluorescence
681.25nm	Chl fluorescence peak, red edge
708.75nm	Chl fluorescence baseline, red edge transition
753.75nm	O2 absorption/clouds, vegetation
761.25nm	O2 absorption/aerosol corr.
764.375nm	Atmospheric corr.
767.5nm	O2A used for cloud top pressure, fluorescence over land
778.75nm	Atmospheric corr./aerosol corr.
865nm	Atmos. corr./aerosal corr. Clouds,
885nm	Atmos. Corr/water vapour absorption band Common reference band with SLSTR
900nm	Water vapour absorption band/vegetation
940nm	Water vapour absorption band, atmos./aerosol corr.
1020nm	Atmos./aerosol corr.

Temporal resolution

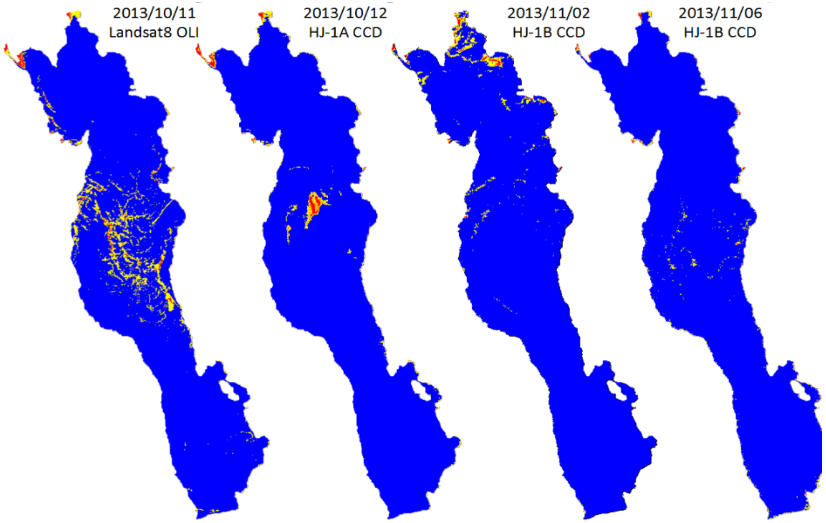

Land	Open Ocean Waters (Case 1 waters)	Coastal and Inland Waters (Case 2 waters)
Sensor Requirements		
Broad spectral bands	Narrow spectral bands	Narrow spectral bands
Wide dynamic range	Narrow dynamic range	Wide dynamic range
Low signal-to-noise	High signal-to-noise	High signal-to-noise
Techniques		
Clustering; classification	Atmospheric correction; pigment algorithm	Radiative transfer; multivariate techniques
Characteristics of Features to be Monitored		
Spatial scales ~10 m	Spatial scales ~1 km	Spatial scales ~ 30 m
Time scales ~ 10 - 100 d	Time scales ~1 d	Time scales ~ 0.2 d
Crisp, fixed boundaries	Fluid boundaries	Fluid boundaries
Many spectral signatures	One spectral signature	Many spectral signatures

Short term goal of flood mapping and monitoring T.C.
Preparing the exploitation Sentinel series

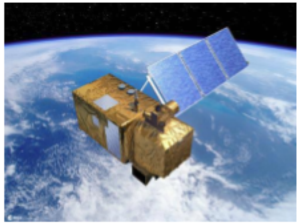

Sentinel 2

- Resolution same as SPOT5 (10m)
- Presence of a SWIR band
- Large swath (MERIS)
- Revisiting time

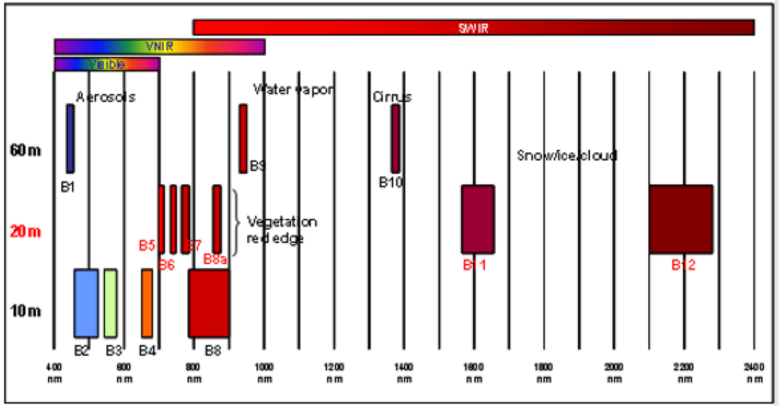

Sentinel 2 observation over Yantgze middle watershed

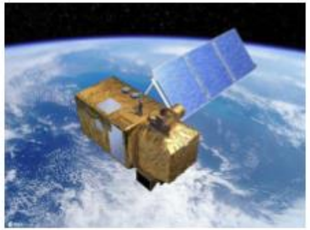

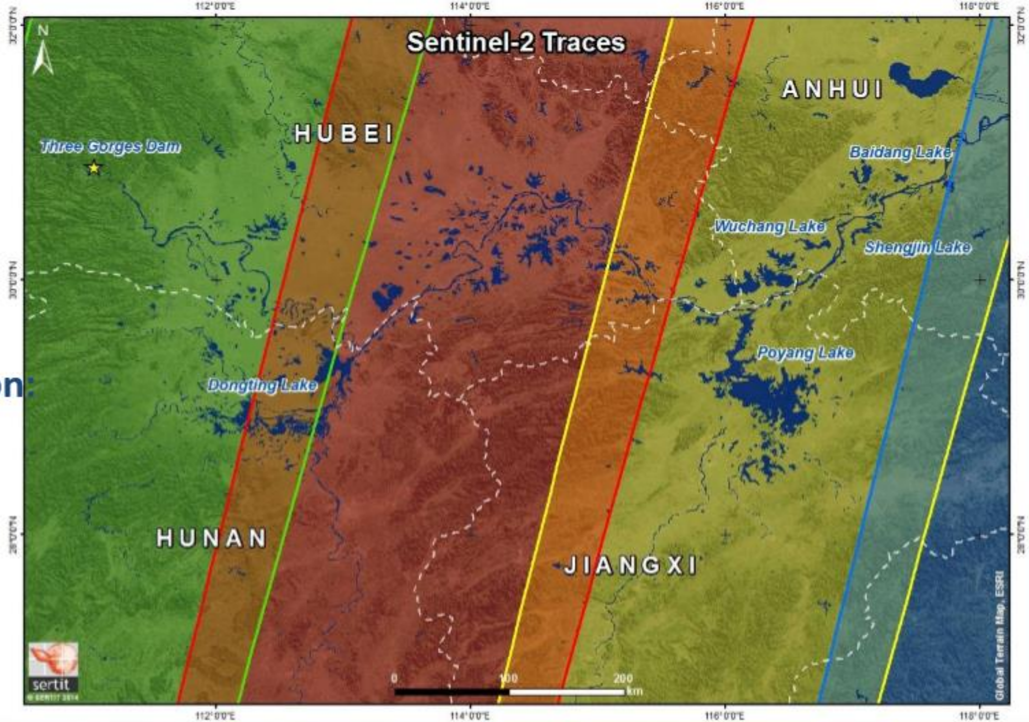

one cycle of acquisition:
Red: Day 3,
Green: Day 6,
Blue: Day 7,
Yellow: Day 10.

Sentinel 2 like: Applicable to others optical sensors

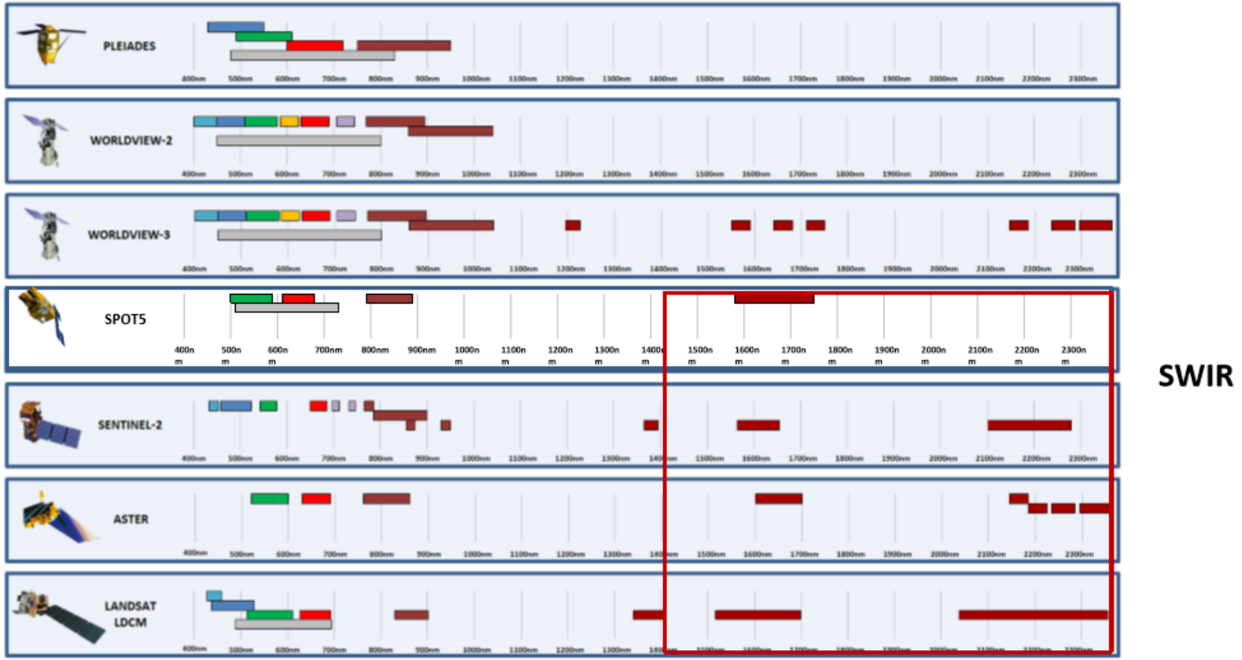

HJ1 A & B constellation

Launched in September 2008
CCD camera (both), a hyper-spectral camera (HJ 1A) or an infrared camera (HJ 1B).

WVC (WIDE View CCD Cameras)

Instrument	CCD detector (pushbroom type)
Spectral bands (4), µm	B1=0.43-0.52, B2=0.52-0.60, B3=0.63-0.69, B4=0.76-0.90
Spatial resolution	30 m
Swath width	360 km x 2 = 720 km (double swath observation provided by parallel camera mounts)

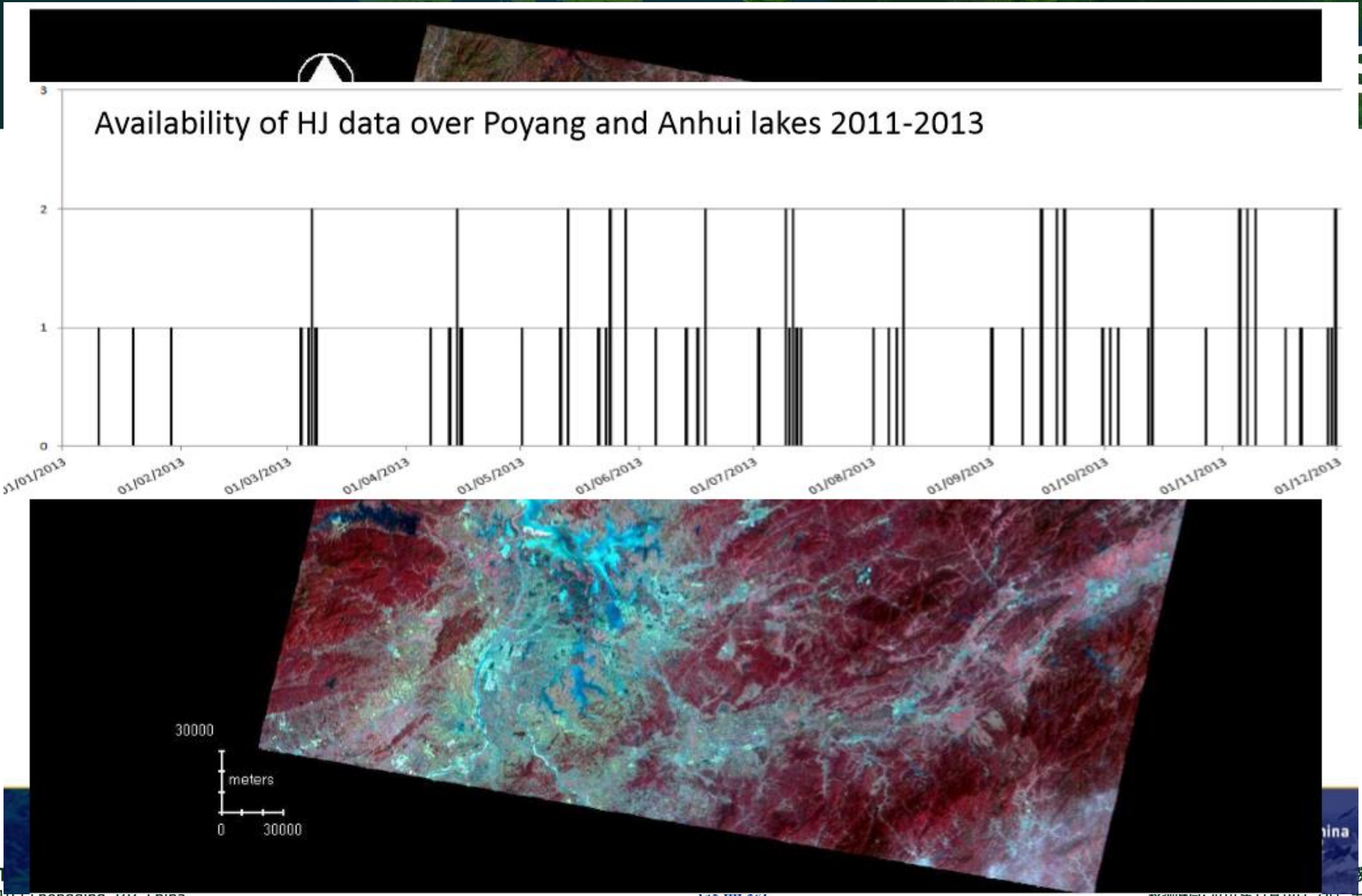
Availability of HJ data over Poyang and Anhui lakes 2011-2013
3
2
1
0
01/01/2013
01/02/2013
01/03/2013
01/04/2013
01/05/2013
01/06/2013
01/07/2013
01/08/2013
01/09/2013
01/10/2013
01/11/2013
01/12/2013
30000
meters
0
30000

Sentinel-3 Sensors

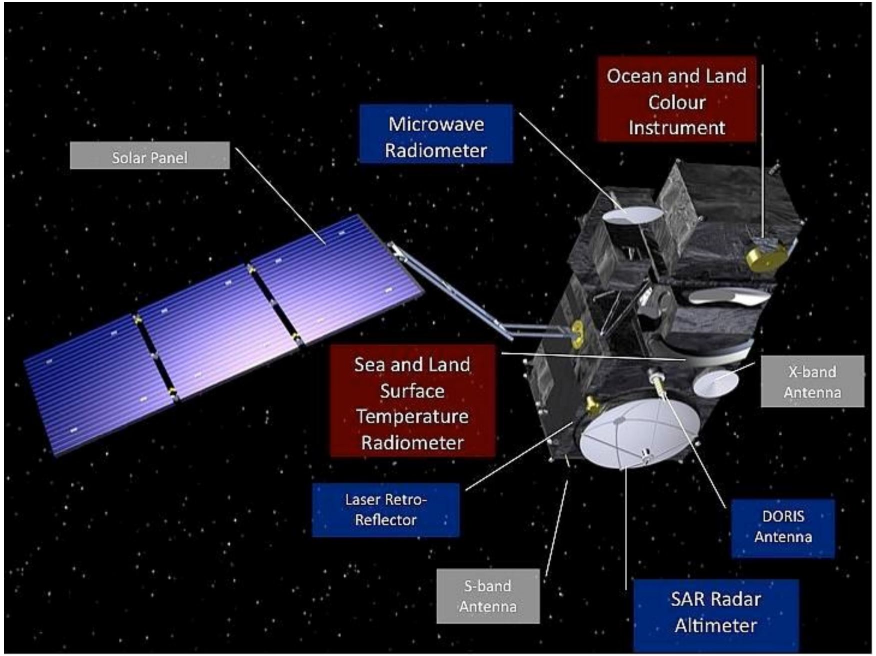

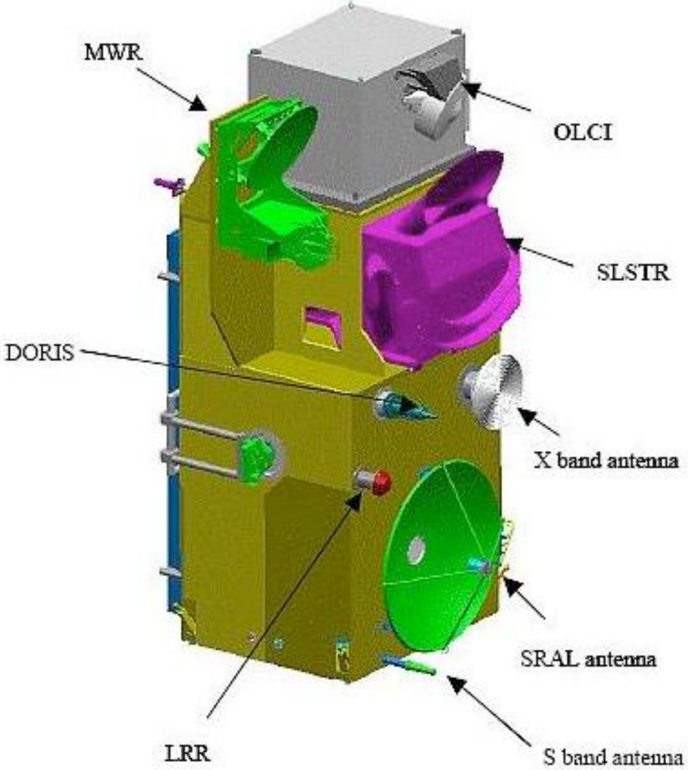

Sensor (Satellite)	MODIS (Terra/Aqua)	MERIS (ENVISAT)	OLCI (Sentinel-3A)	TM/ETM+ (Landsat-5/7)	OLI (Landsat-8)	MSI (Sentinel-2A/B)	CCD (HJ-1A/B)
Agency	USA	Europe	Europe	USA	USA	Europe	China
Working time	1999-Now	2002-2012	2016-Now	1984-2011/ 1999- Now	2013-Now	2015-Now 2017-Now	2008-Now
Spatial resolution(m)	250/500/100	300	300	30	30	10/20/60	30
Repeat days	1	3	2	16	16	5(A+B)	2(A+B)
bands	36	15	21	7/8	9	13	4
Swath(km)	2330	1150	1270	180	180	290	360
orbit	Polar	Polar	Polar	Polar	Polar	Polar	Polar
Spectral Coverage(μm)	0.4-14.38	0.407-0.905	0.39-1.06	0.45~2.35	0.43-2.3	0.443-2.19	0.43-0.9

MODIS (1000m)	MERIS	OLCI	Function
		400nm	Aerosol correction, improved retrieval
412.5nm	412.5nm	412.5nm	Yellow substance(turbidity)
443nm	442.5nm	442.5nm	Chl absorption max
488nm	490nm	490nm	High Chl, other pigments
	510nm	510nm	CHL, sediment, turbidity, red tide
531nm	560nm	560nm	Chl absorption min
551nm	620nm	620nm	Sediment
667nm	665nm	665nm	Chl(2nd Chl abs. max), sediment, yellow substance
		673.35nm	Improved fluorescence
678nm	681.25nm	681.25nm	Chl fluorescence peak, red edge
	705nm	708.75nm	Chl fluorescence baseline, red edge transition
748nm	753.75nm	753.75nm	O2 absorption/clouds, vegetation
	760nm	761.25nm	O2 absorption/aerosol corr.
		764.375nm	Atmospheric corr.
		767.5nm	O2A used for cloud top pressure, fluorescence over land
	775nm	778.75nm	Atmospheric corr./aerosol corr.
869.5nm	865nm	865nm	Atmos. corr./aerosal corr. Clouds,
	890nm	885nm	Atmos. Corr/water vapour absorption band Common reference band with SLSTR
905nm	900nm	900nm	Water vapour absorption band/vegetation
936nm		940nm	Water vapour absorption band, atmos./aerosol corr.
		1020nm	Atmos./aerosol corr.

Mission capability

Algorithms

In-situ observations

Operational capability

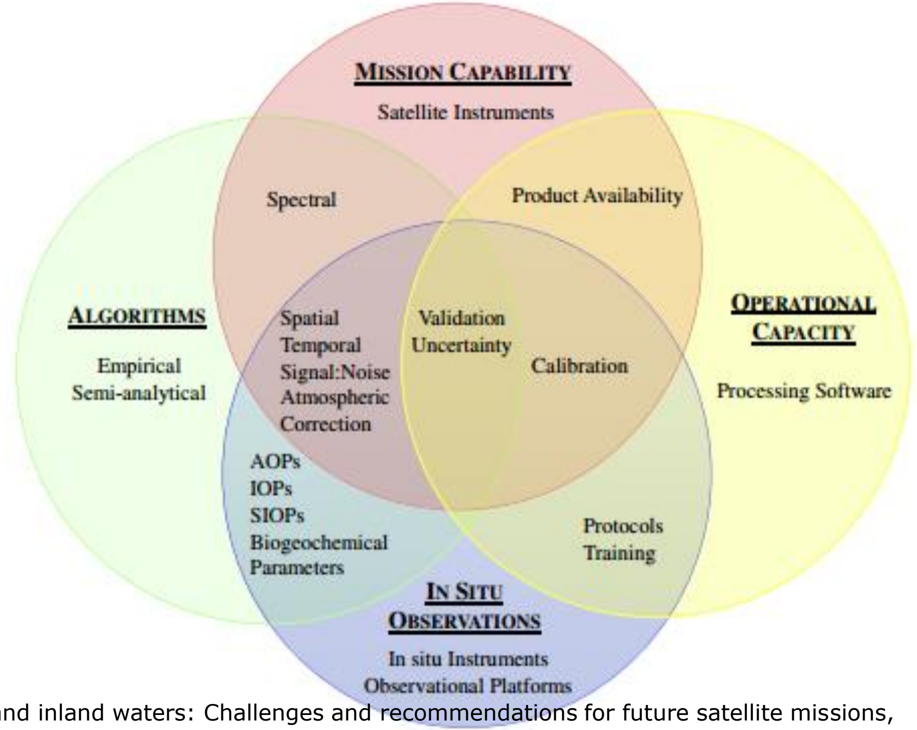

Colleen B. Mouw，2015, Aquatic color radiometry remote sensing of coastal and inland waters: Challenges and recommendations for future satellite missions, Remote sensing and environment

Atmospheric correction

Molecular

Aerosol

Sea-atmosphere surface

Sun glint

Water components retrieval

Inorganic suspended material

Phytoplankton

CDOM (colored dissolve organic matters)

Bottom effects

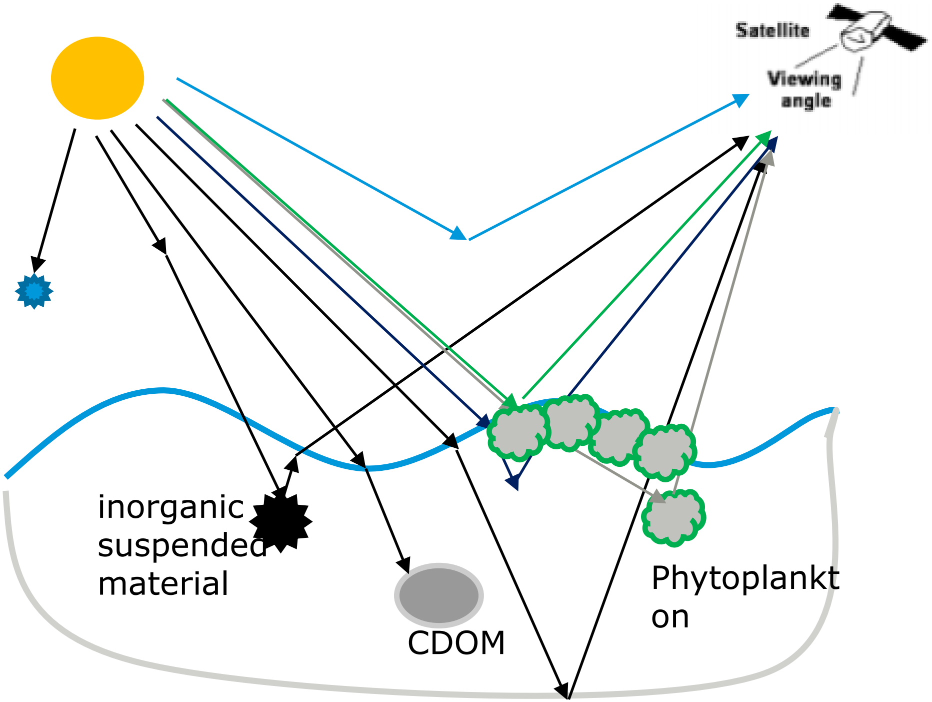

Geometric correction with a high accuracy

Atmospheric correction under high aerosol optical depth(AOD) and high water-leaving reflectance in NIR bands

Water components retrieval algorithms with correctly description of radiative transfer model

Validation and uncertainty evaluation

Atmospheric Correction (AC) and Inherent Optical Properties (IOP) Processor for Sentinel 3, MERIS, MODIS, SeaWiFS Level 1b radiance products

Brockmann C. et al. 2016, Evolution of the C2RCC neural network for sentinel 2 and 3 for the retrieval of ocean colour products in normal and extreme optically complex waters , ‘Living Planet Symposium 2016’, Prague, Czech Republic

APPLICATIONS

Water body

Flood mapping based on thresholding of raw channel and /or indice

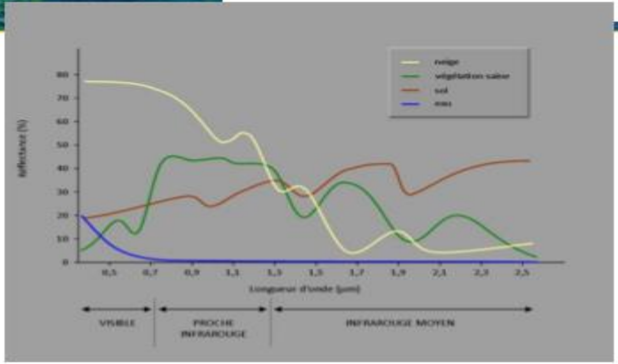

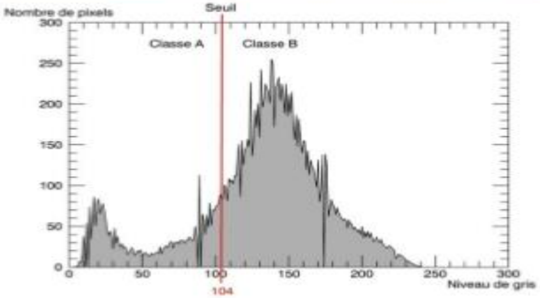

Fundamentals: : water areas can be very bright if containing suspended materials

Extraction of water bodies from:

- **Brightness Standard or Tasseled Cap**
- **First component of a PCA,**
- **Saturation indices of a HIS transformation**

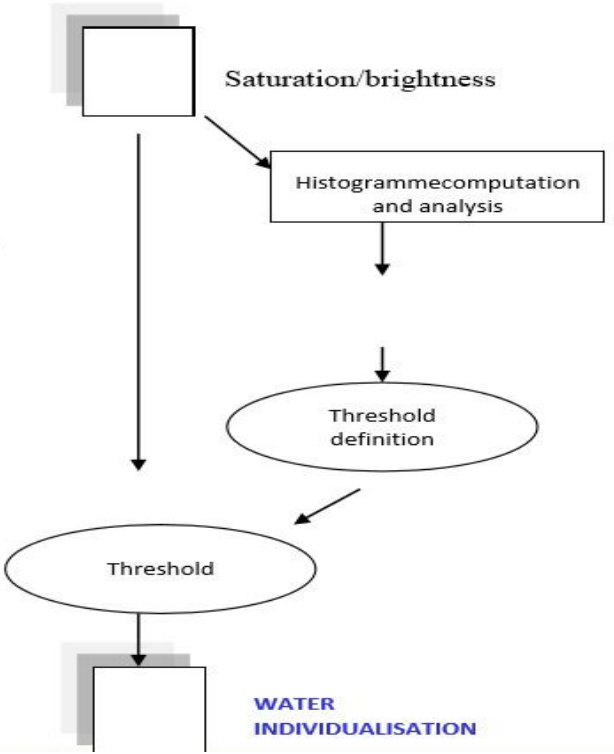

FAI

$$R'_{rc,NIR} = R_{rc.RED} + \left(R_{rc,SWIR} - R_{rc,RED}\right) \times \frac{\lambda_{NIR} - \lambda_{RED}}{(\lambda_{SWIR} - \lambda_{RED})}$$

$$R_{rc,NIR} = \frac{\pi {L_t}^*}{F_0 cos\theta_0} - R_r$$

$$FAI = R_{rc,NIR} - R'_{rc,NIR}$$

L'_t is the calibrated sensor radiance after adjustment for ozone and other gaseous absorption;
F_0 is the extraterrestrial solar irradiance at data acquisition time;
θ_0 is the solar zenith angle;
R_r is Rayleigh reflectance estimated with 6S

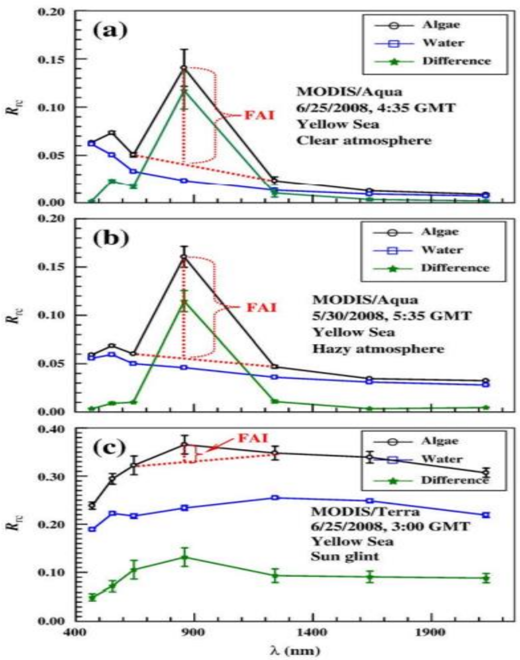

$$FAI = R_{rc}(NIR) - R_{rc}(RED) + \left(R_{rc,}(RED) - R_{rc}(SWIR)\right) \times \frac{NIR - RED}{SWIR - RED}$$

Inundation Areas for Each Year between 2000 and 2010

Using FAI (Floating Algae Index) and a gradient method to delineate inundation area. 620 MODIS cloud free images were selected between 2000 and 2010.

Intra-annual changes: a factor of 2.3 – 3.2

Maximum possible inundation was 14 times larger than minimum inundation

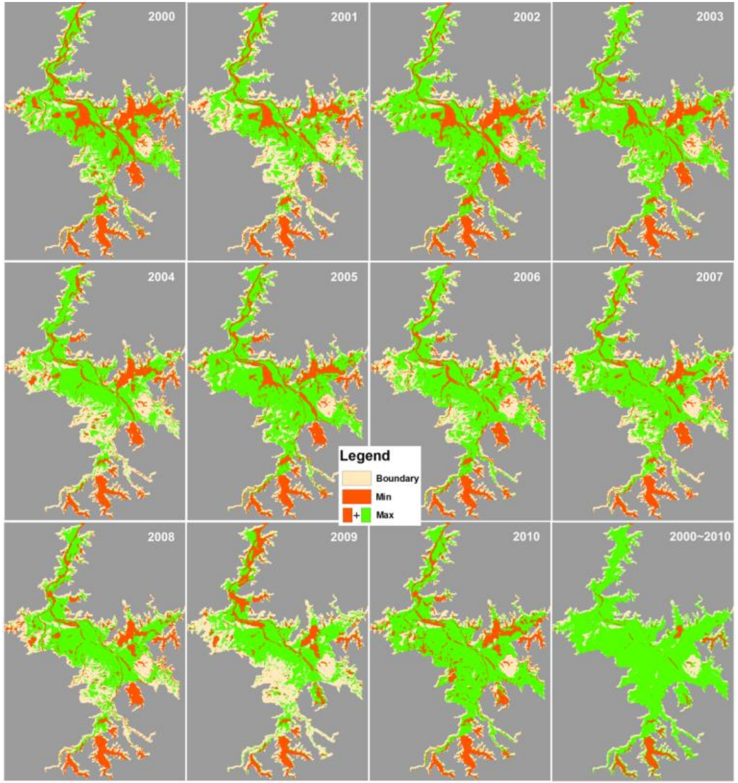

Inundation Areas for Each Month between 2000 and 2010

● The monthly min inundation area between September and March is only <50% of that between June and July
● The monthly max inundation area is significantly lower during December to January
●From June to August, >50% of the Poyang lake region was inundated even at minimal inundation
● Max/min ratios range between 1.46 (June) to 4.03 (October), suggesting significant inter-annual variability for all months
● A dramatic decline in the monthly minimum inundation occurred between August and September (from 1706.6 to 832.1 km^2), leading to a sharp increase in the max/min ratio (from 1.85 to 3.64)

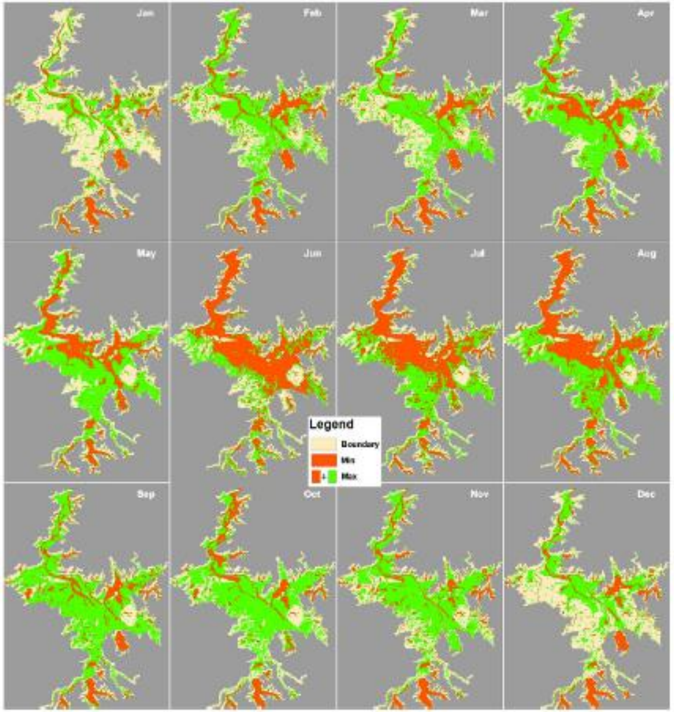

Month		Jan	Feb	Mar	Apr	May	Jun	Jul	Aug	Sep	Oct	Nov	Dec
Maximum	Area	1705.9	2665.8	2561.2	2861.6	3038.5	2820.1	3052.1	3162.9	3025.5	2864.7	2768.5	1960.1
	Year	2003	2005	2010	2010	2010	2003	2010	2010	2002	2010	2000	2002
Minimum	Area	797.3	958.9	888.7	1020.8	1120.3	1931.8	1819.1	1706.6	832.1	710.7	812.3	824.5
	Year	2006	2007	2008	2007	2007	2004	2009	2001	2006	2009	2009	2007
Max/Min Ratio		2.14	2.78	2.88	2.8	2.71	1.46	1.68	1.85	3.64	4.03	3.41	2.38

Inundation area of May 2011 (red),overlaid on the mean inundation area during May 2000-2010 (green)

✓ A serious drought in 2007 triggered potable water problems for more than ten million people
✓ A big flood event in 1998 resulted in economic losses of more than 30 billion Yuan in the Poyang Lake region

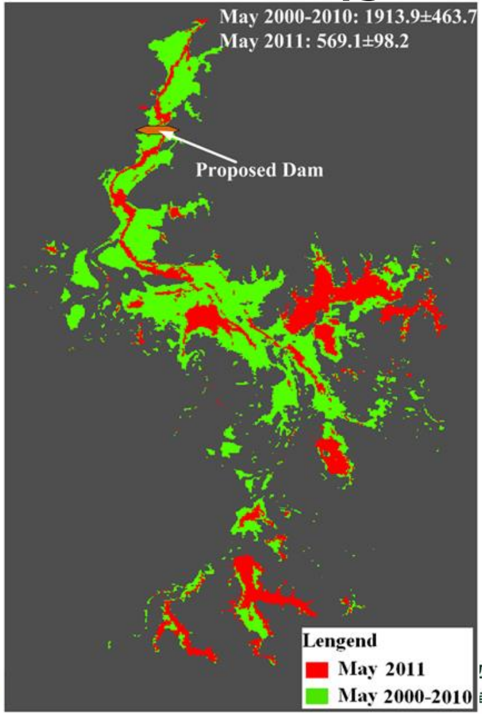

Bottom topography of Poyang Lake

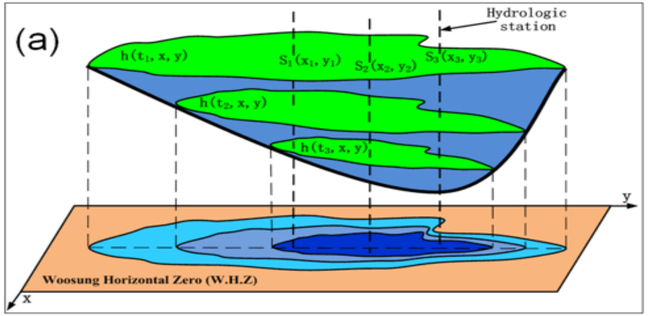

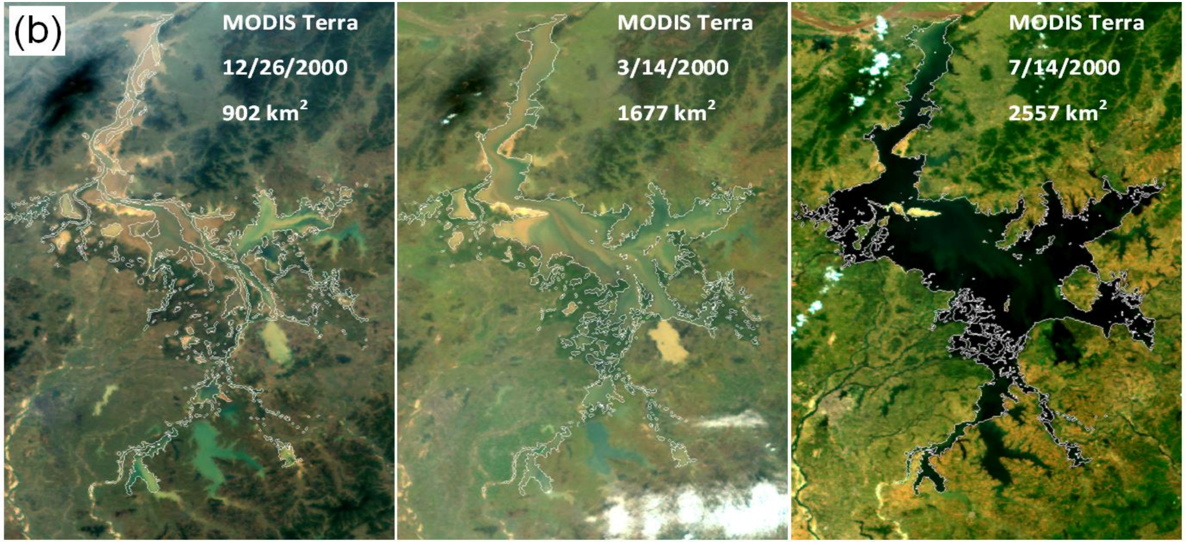

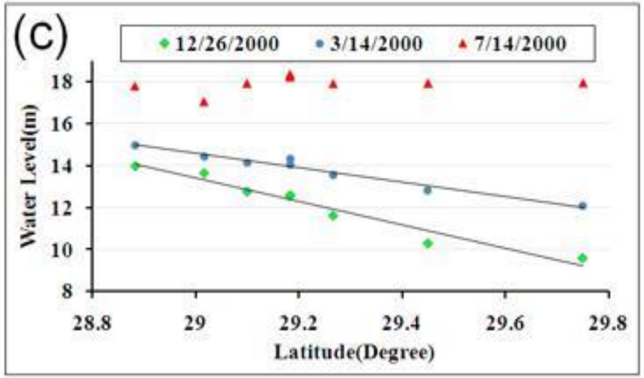

Bottom topography of Poyang Lake

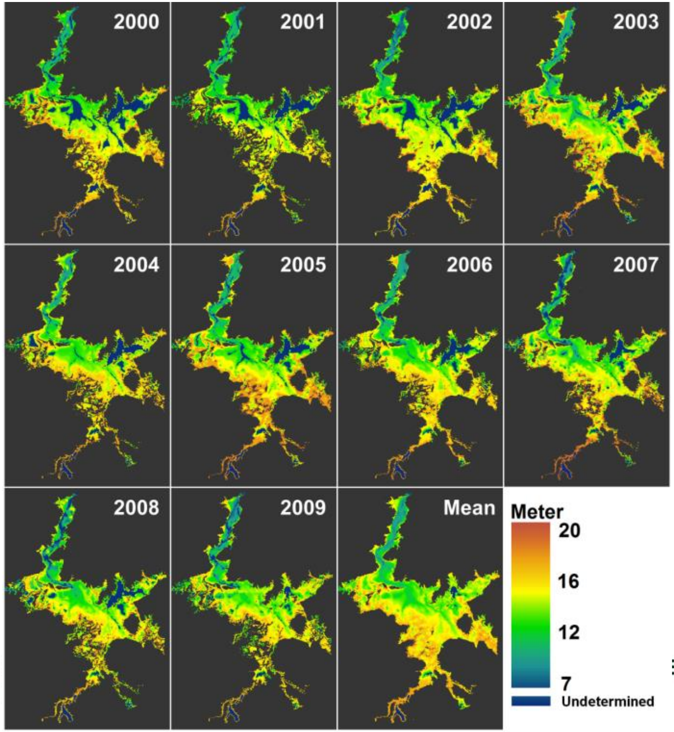

The lake bottom has an typical elevation of 12–17 m (around 80%)

Agree well with in-situ measurements

Inundation area & water volume of Poyang Lake: 2000-2009

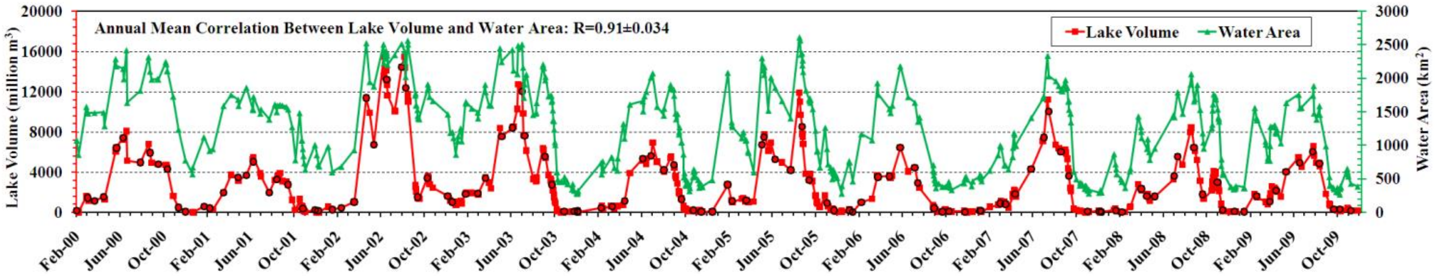

Water budget of Poyang Lake: 2000-2009

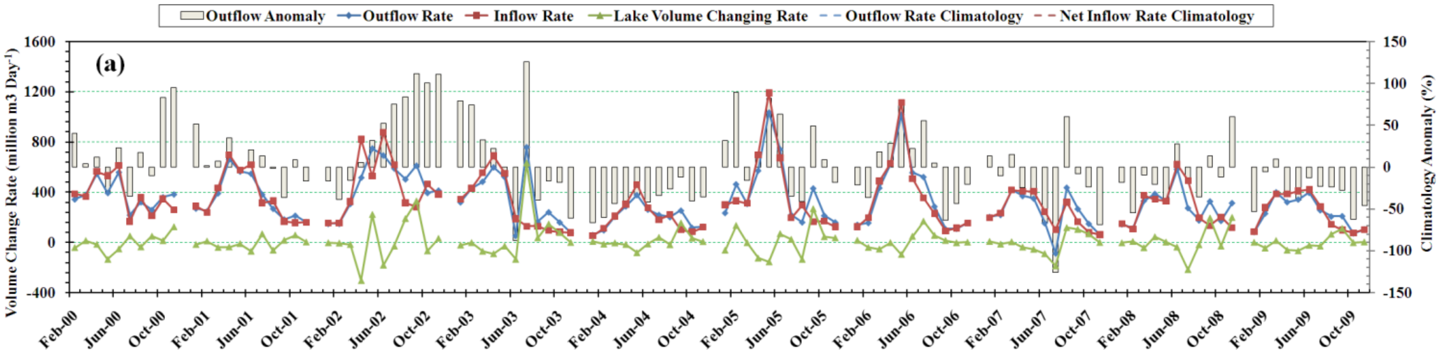

APPLICATIONS
Wetland

15 years Vegetation community transitions in Poyang Lake wetland

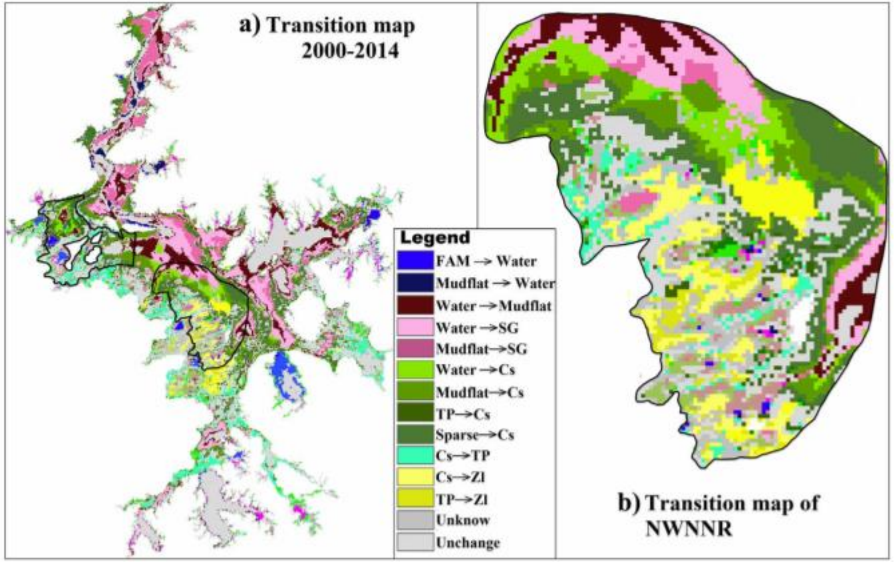

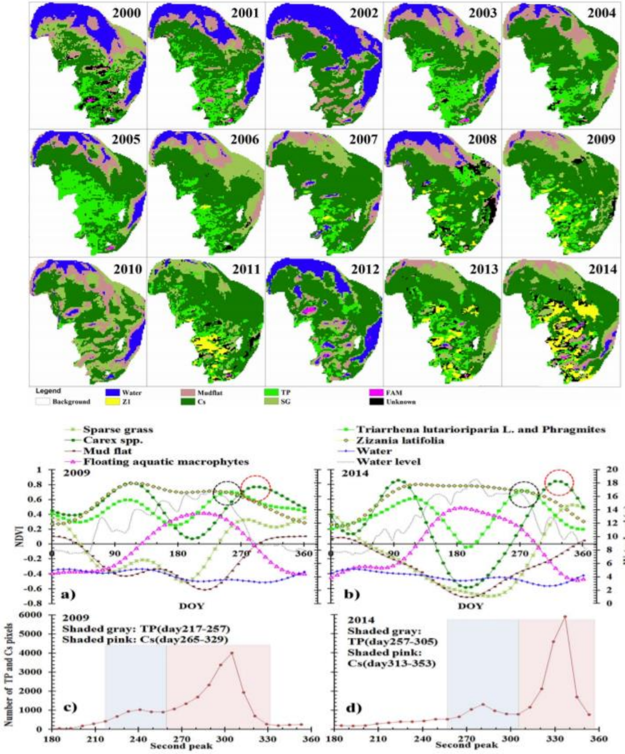

Xingxing Han, Lian Feng, Chuanmin Hu and Xiaoling Chen, Wetland changes of China's largest freshwater lake and their linkage with the Three Gorges Dam, Remote Sensing of Environment

Method: Spectral and temporal features of different vegetation categories

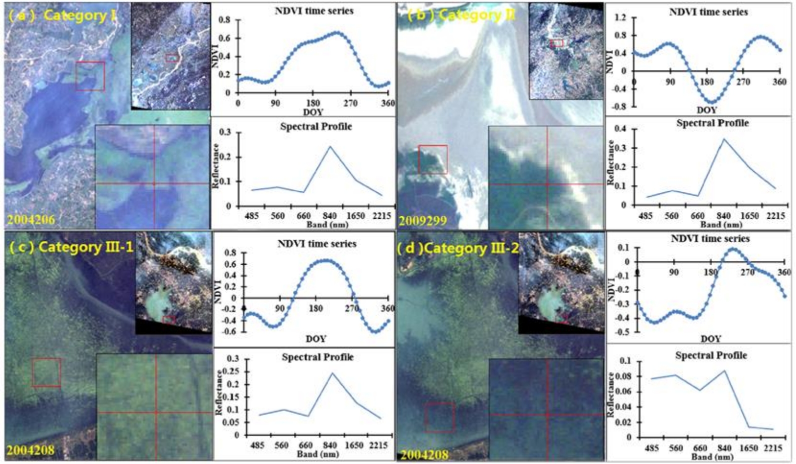

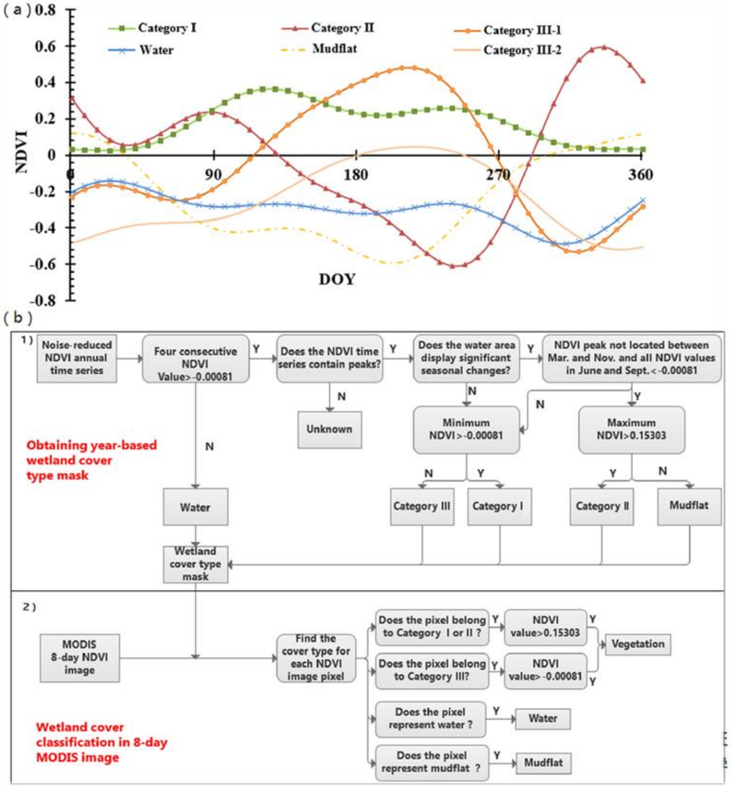

- Few differences were found in the satellite derived spectral profiles for different wetland vegetation in Yangtze Plain. However, the annual NDVI changes of wetland vegetation could generally fall into three categories, large differences could be found in the occurred time of NDVI increasing trend and the maximum or minimum NDVI value in the NDVI time series.

Results 1: Spatial and temporal distribution of wetland vegetation

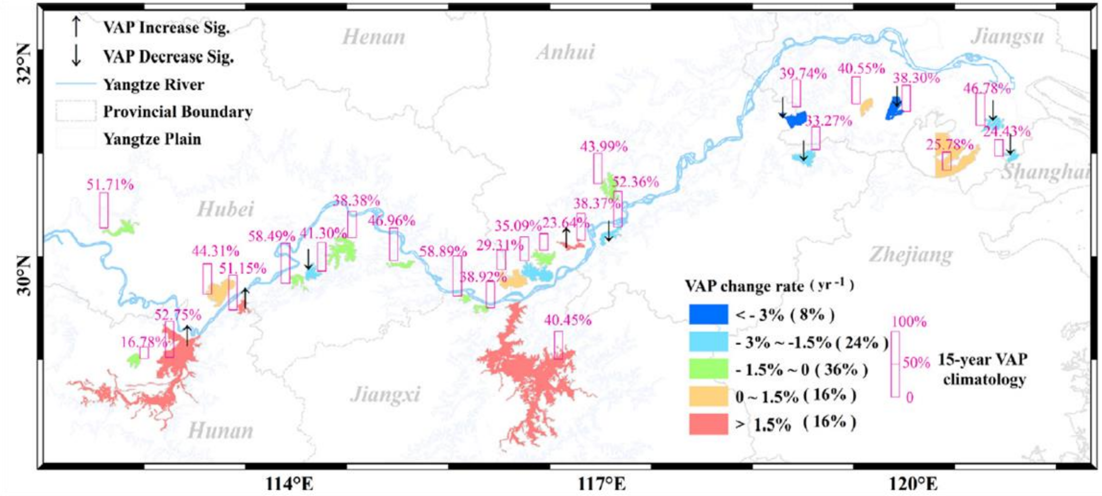

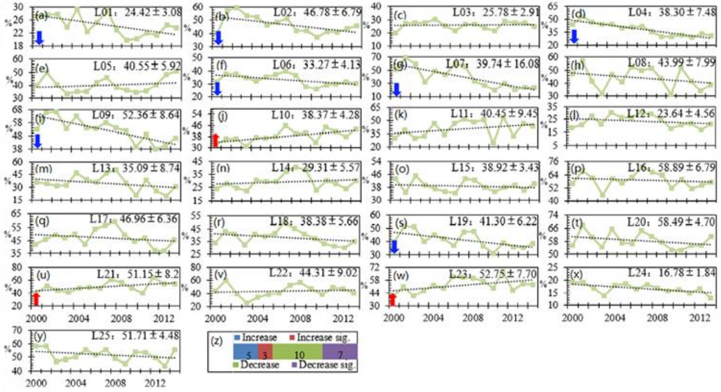

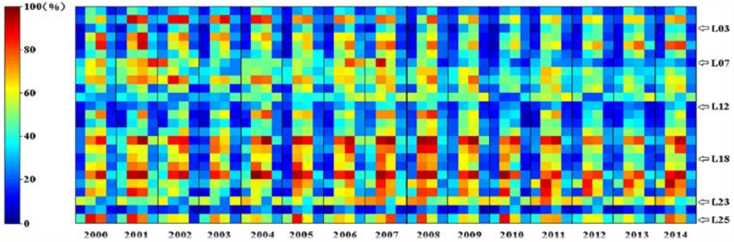

- The coverages of wetland vegetation accounted for 16.78% to 58.89% of the total areas of these 25 lakes during the period 2000 to 2014.
- More than half of the lakes (17/25) showed decreasing trends in their vegetation area percentage (VAP),

- Differences of seasonal change in VAPs of lakes were found. The maximum VAPs typically occurred in the second and third quarters, minimum VAPs were observed in the first and fourth quarter.

Hou X, Chen X, Liu W, et al., Changes in the wetland vegetation growth patterns in large lakes on the Yangtze Plain. International Journal of Remote Sensing, 2019,40(11): 1-12

- 44% of the lakes have 15-year mean greenness values of<0.2, 52% were between 0.2 and 0.3, and 4% were>0.3.
- Over half of the lakes (17/25) have demonstrated decreasing trends in their greenness values over the period.

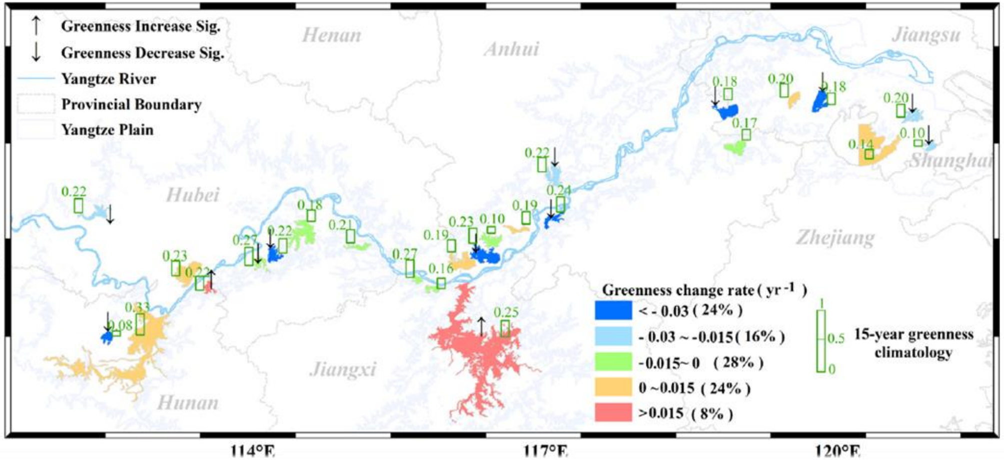

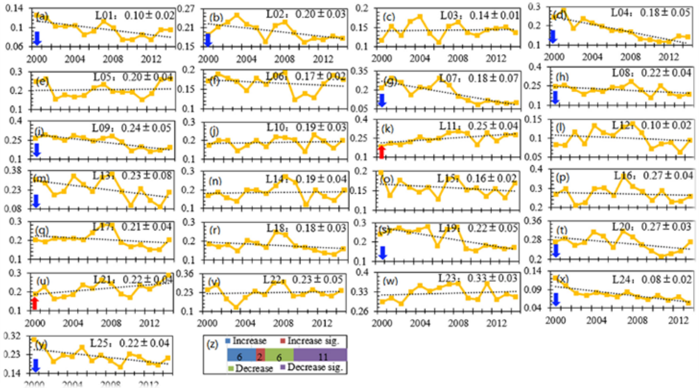

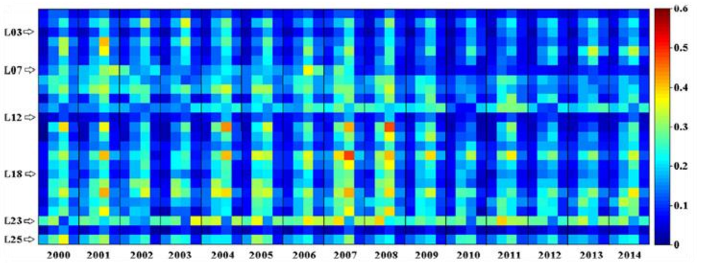

Results 2: Phenology change of wetland vegetation

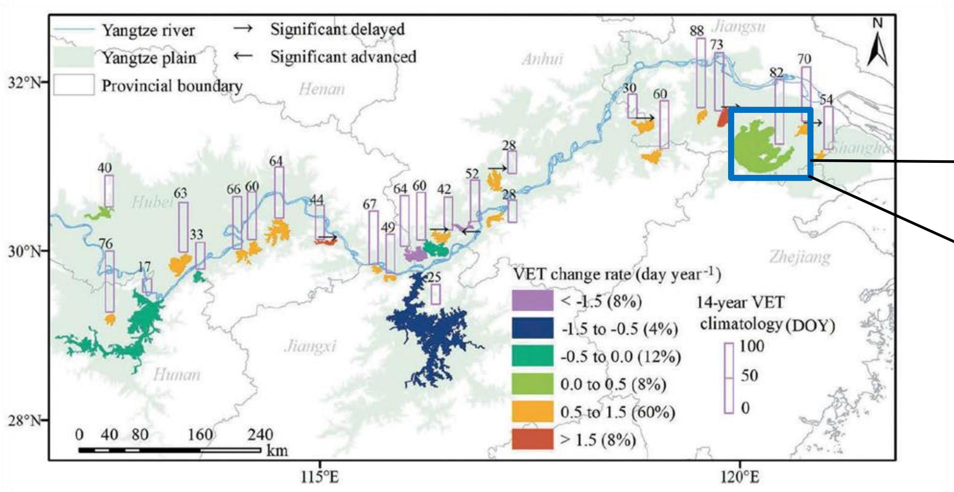

- 76% of the lakes showed delayed trends in the vegetation emergence times (VET), and 32% of them were statistically significant. In contrast, 24% of the lakes displayed advanced trends in the VET and 17% of them were statistically significant over the past 14 years.

- The VET of Taihu lake mainly occurred between 1 and 60 (i.e. January to February) for most regions. The VET of eastern Taihu Lake exhibited a delayed trend.

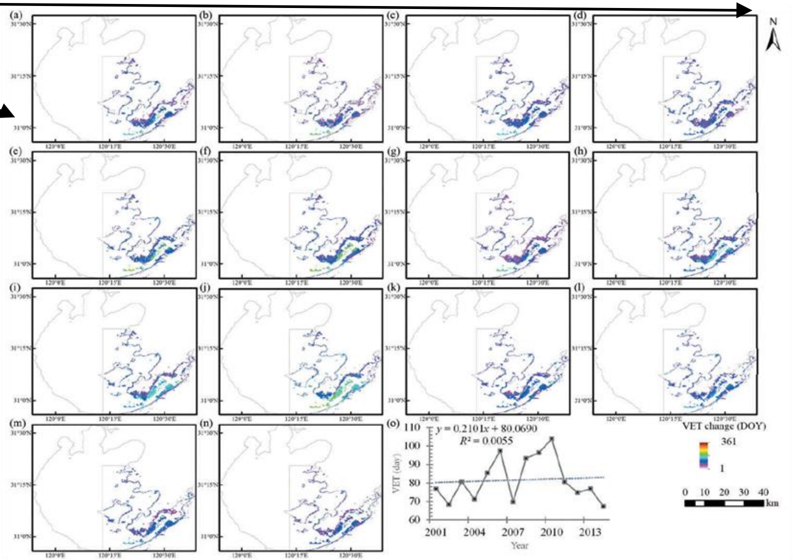

Results 3：Driving forces analysis

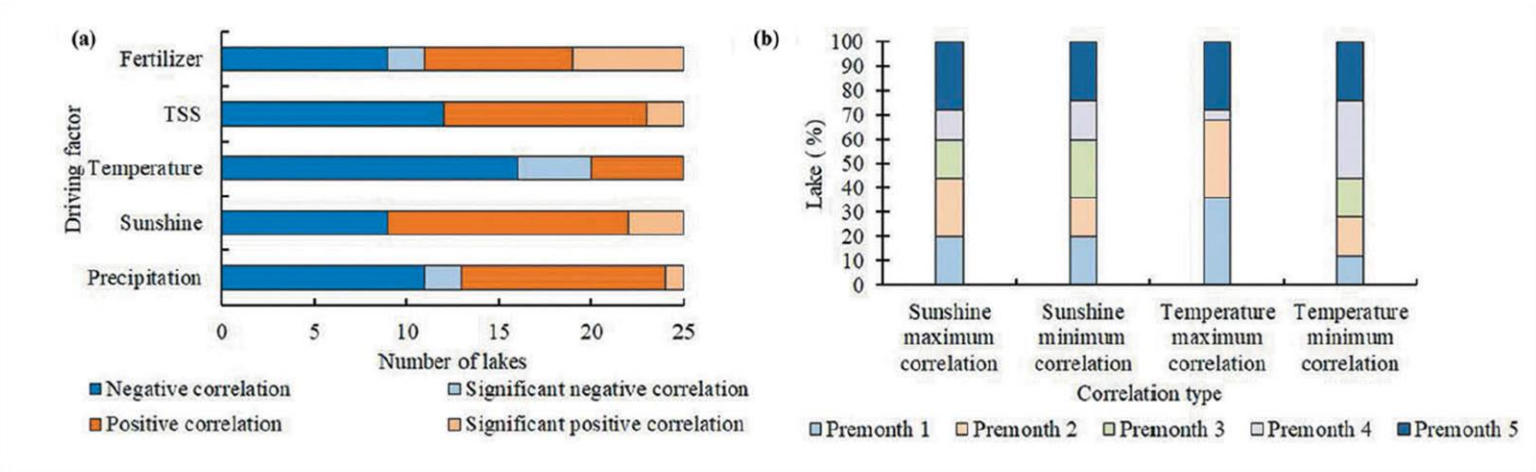

- The amounts of chemical fertilizers used in nearby farmlands have played an important role in influencing the vegetation growth for some of the lakes.
- VET change was more sensitive to temperature and sunshine duration than to precipitation for most of the lakes. The temperature in 1–2 months before VET had great effect on the vegetation growth, while such a pattern was not evident for sunshine duration for 5 months before VET.

Hou, X., Feng, L., Chen, X., & Zhang, Y. Dynamics of the wetland vegetation in large lakes of the Yangtze Plain in response to both fertilizer consumption and climatic changes. ISPRS Journal of Photogrammetry and Remote Sensing, 2018,141: 148-160

APPLICATIONS

Eutrophication

What is Eutrophication?

Eutrophication refers to the Enrichment of a water body with Nutrients, usually with an excess amount of nutrients.

Algal bloom is one of the results.

Eutrophication ≠ algae bloom

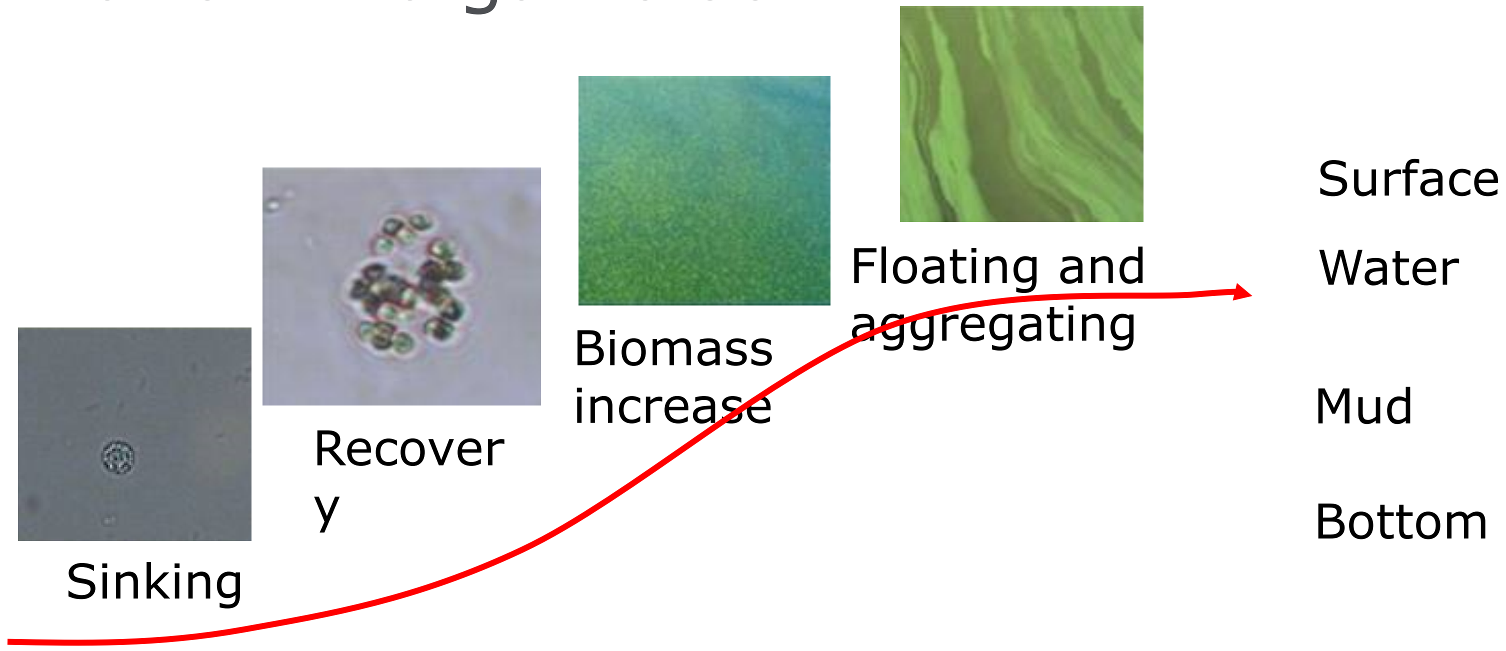

Ronghua Ma, Harmful algae blooms, 2017, Summer school of ocean color remote sensing in China: theory and application

Eutrophication in Lakes now become world wild and frequency

Cyanophyta
Algae
clustering
Near shore

Bacillaeiophyta
Small algal
blooms
Southeast and
North area

Cyanophyta
blooms
First record
Whole Lake

Cyanophyta
blooms
Multi times,
Long lasting
Whole lake

1990 1996 2003 2016

Radiative resolution

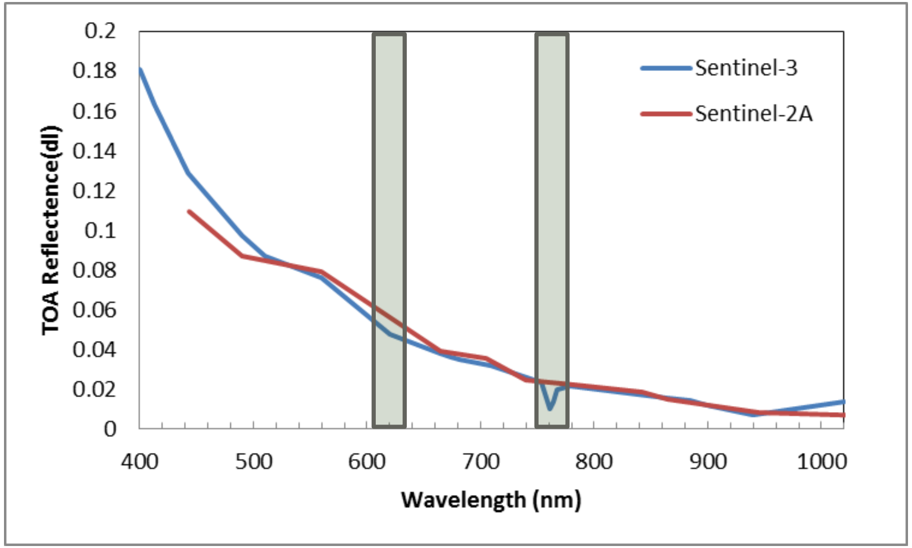

OLCI	Function
400nm	Aerosol correction, improved retrieval
412.5nm	Yellow substance(turbidity)
442.5nm	Chl absorption max
490nm	High Chl, other pigments
510nm	CHL, sediment, turbidity, red tide
560nm	Chl absorption min
620nm	Sediment
665nm	Chl(2nd Chl abs. max), sediment, yellow substance
673.35nm	Improved fluorescence
681.25nm	Chl fluorescence peak, red edge
708.75nm	Chl fluorescence baseline, red edge transition
753.75nm	O2 absorption/clouds, vegetation
761.25nm	O2 absorption/aerosol corr.
764.375nm	Atmospheric corr.
767.5nm	O2A used for cloud top pressure, fluorescence over land
778.75nm	Atmospheric corr./aerosol corr.
865nm	Atmos. corr./aerosal corr. Clouds,
885nm	Atmos. Corr/water vapour absorption band Common reference band with SLSTR
900nm	Water vapour absorption band/vegetation
940nm	Water vapour absorption band, atmos./aerosol corr.
1020nm	Atmos./aerosol corr.

Remote Sensing for Sediment Retrieval

Water reflectance ~0 at >1000 nm

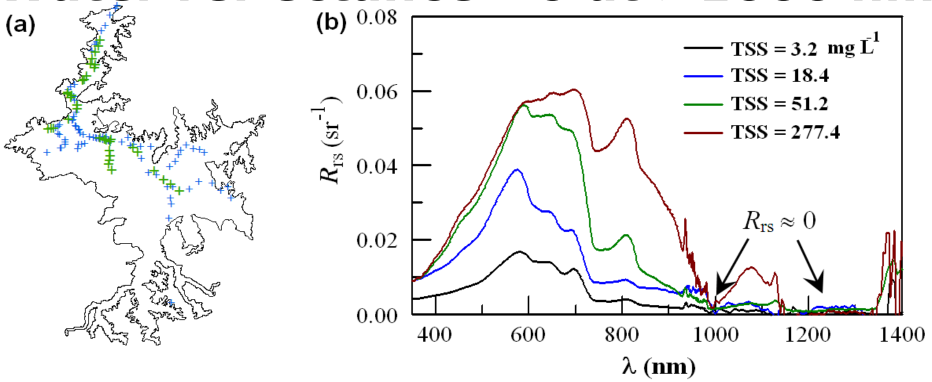

645 nm "immune" to land adjacency effect

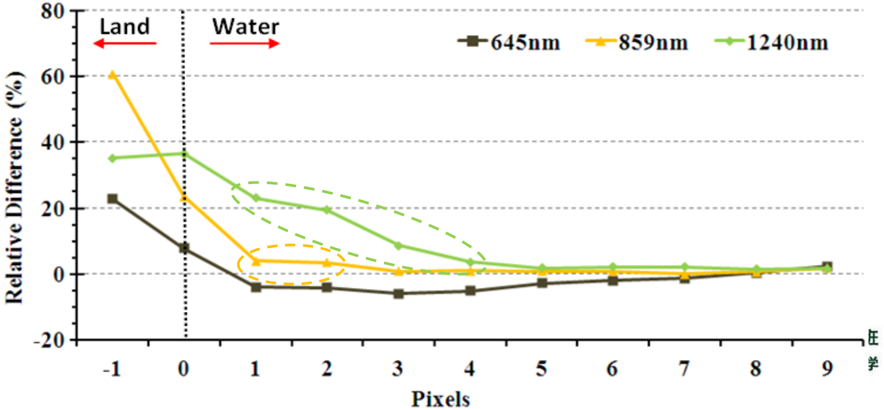

Retrieval algorithm development:
Single band or band ratio?

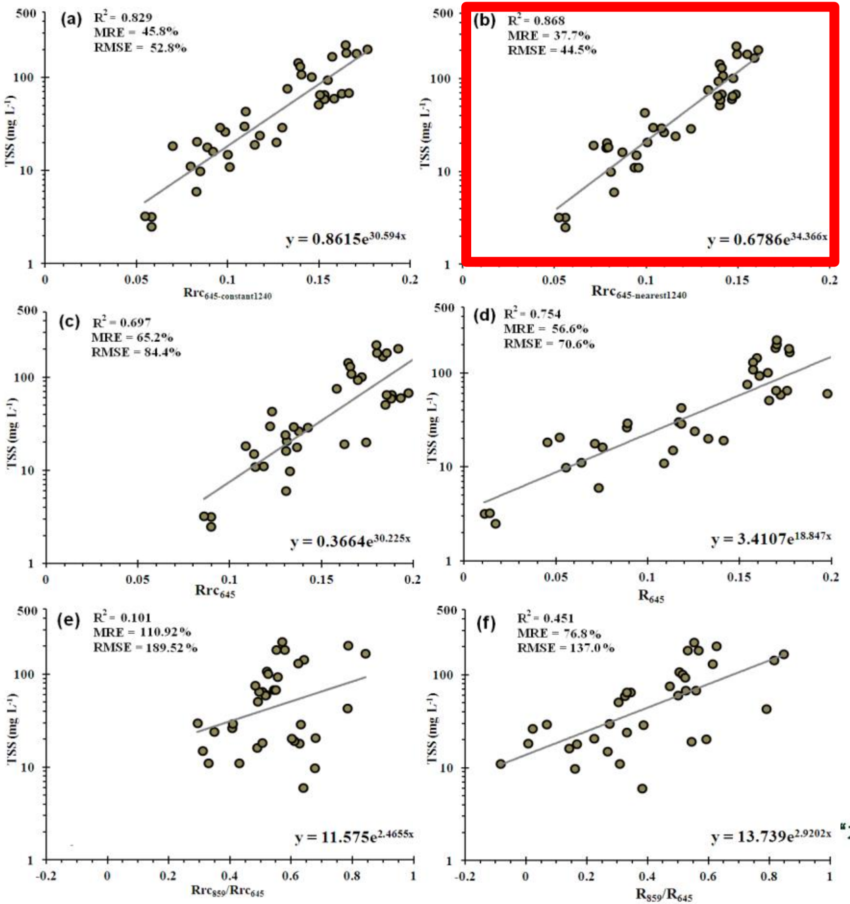

Spatio-temporal Pattern of Suspended Sediments

- Annual mean TSS distributions of Poyang Lake from 2000 to 2010

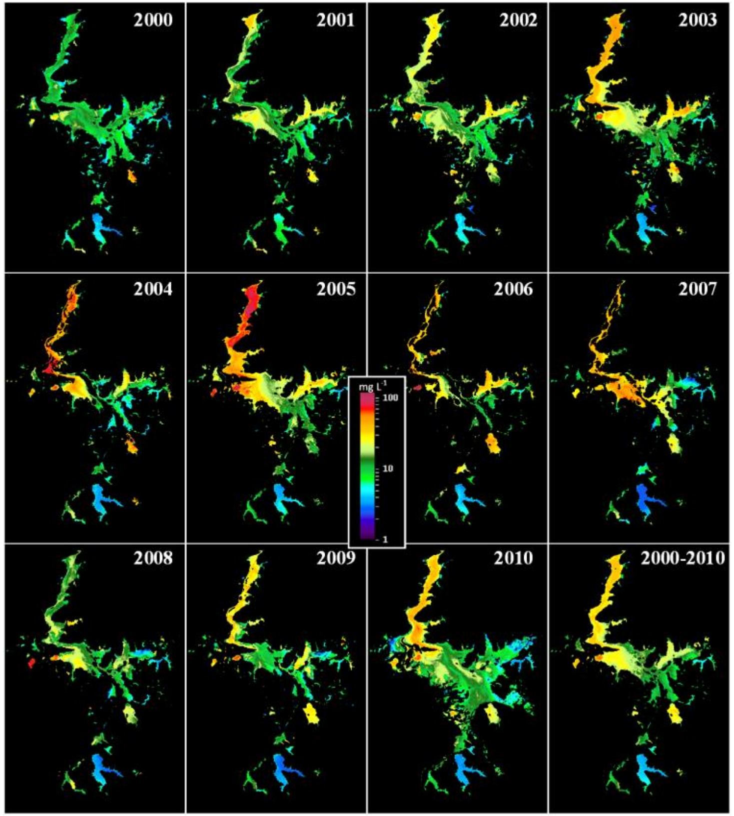

Remote Sensing for Chlorophyll-a Retrieval Using MERIS

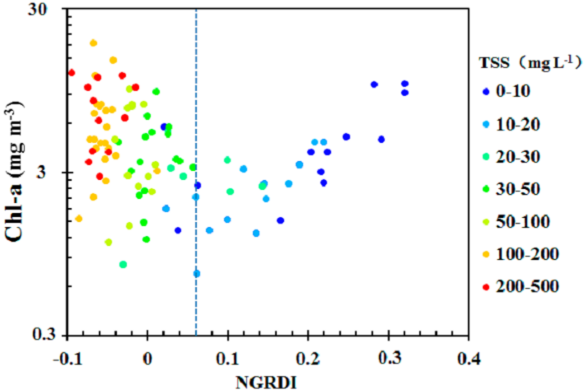

A positive correlation exists between Chl-a and NGRDI in relatively sediment-poor waters.

645 nm "immune" to land adjacency effect

normalized green-red difference index (NGRDI = (Rrs,560 −Rrs,681)/(Rrs,560+ Rrs,681))

Spatio-temporal Pattern of Chlorophyll-a

- Mean Chl-a distributions of Poyang Lake between July and September from 2003 to 2011.
- Higher Chl-a was observed in the small sub-lake in the south and in the astern Poyang Lake.

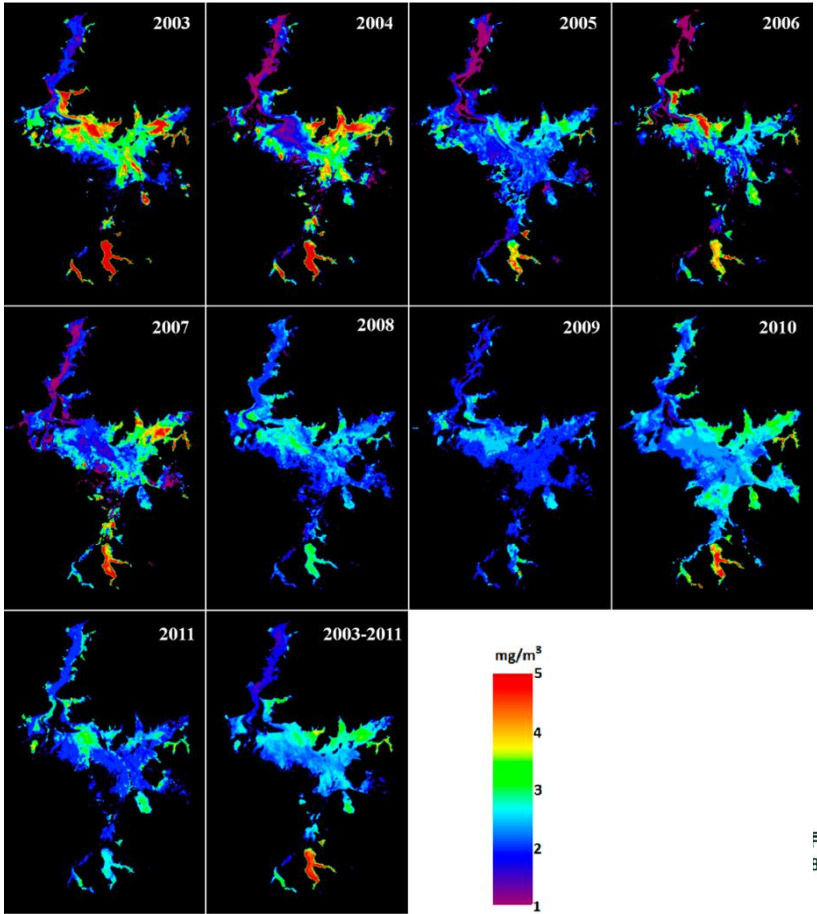

- Chl-a distributions during each climatological month between 2003 and 2012.
- Higher Chl-a was observed in the south, especially for the small sub-lake.
- Chl-a in the summer months appeared higher than in other months.

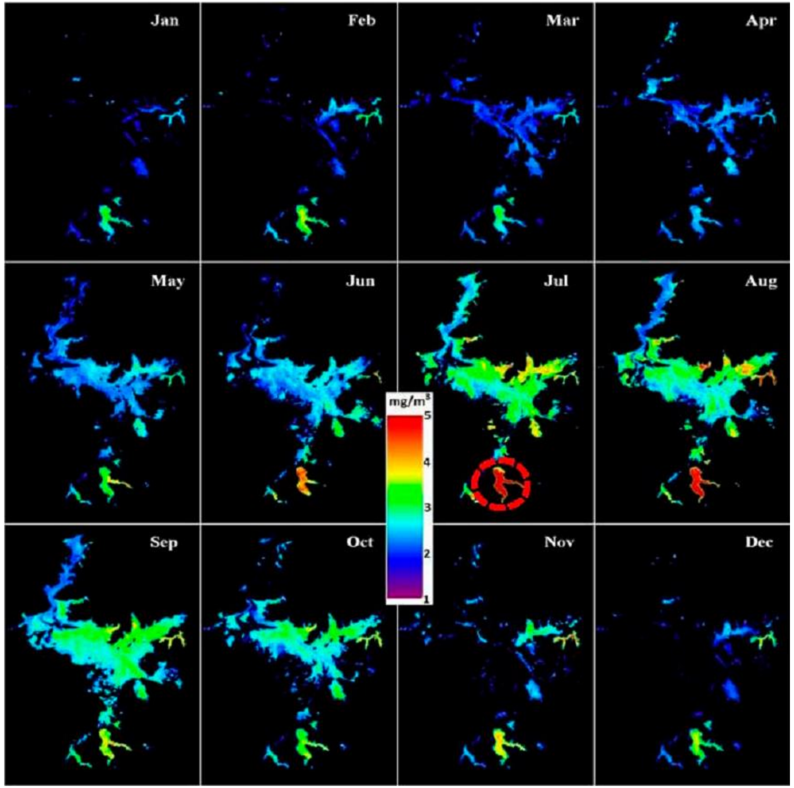

	Jan	Feb	Mar	Apr	May	Jun	Jul	Aug	Sep	Oct	Nov	Dec	Annual Mean
Mean	2.6	2.9	2.5	2.4	3.0	3.4	4.4	4.2	3.5	3.3	3.3	2.9	3.2
Std.	0.5	0.6	0.4	0.2	0.4	0.8	1.0	1.0	0.3	0.3	0.6	0.6	0.6

Mean Chl-a distributions of Erhai Lake from 2003 to 2009

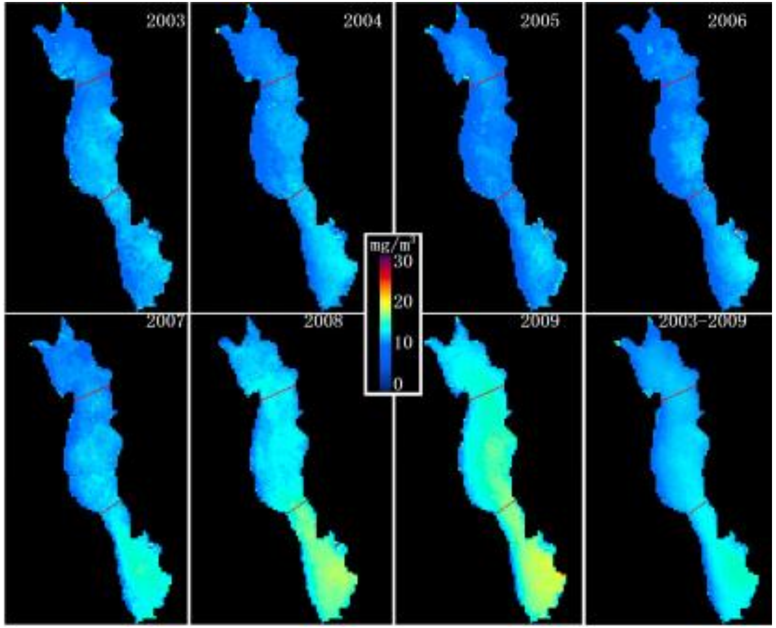

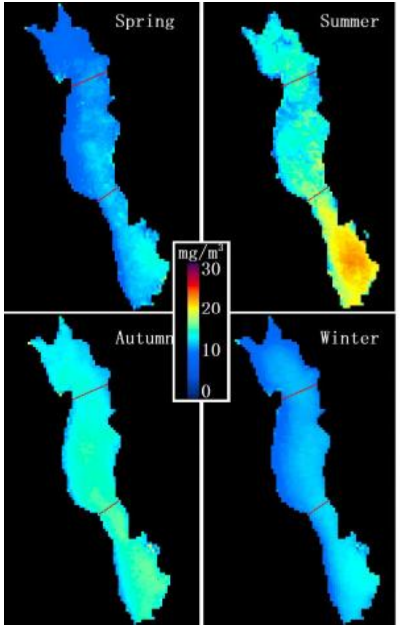

Annually mean Chl-a concentration in Erhai Lake various from 2.1 to 27.8 ug/L

Higher Chl-a was observed in the south, especially after 2007

Chl-a in the summer months appeared higher than in other months.

Han X. et al (2014) MERIS observations of chlorophyll-a dynamics in Erhai Lake between 2003 and 2009, International Journal of Remote Sensing , DOI: 10.1080/01431161.2014.985395

Algal blooms

Identify algal and non-algal waters

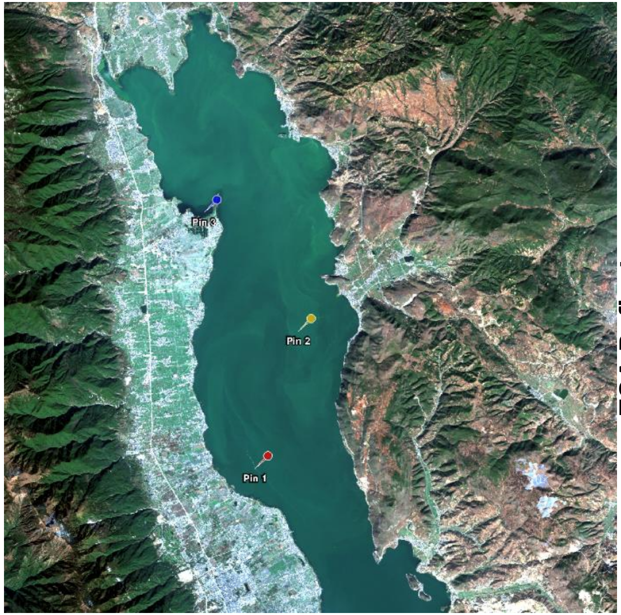

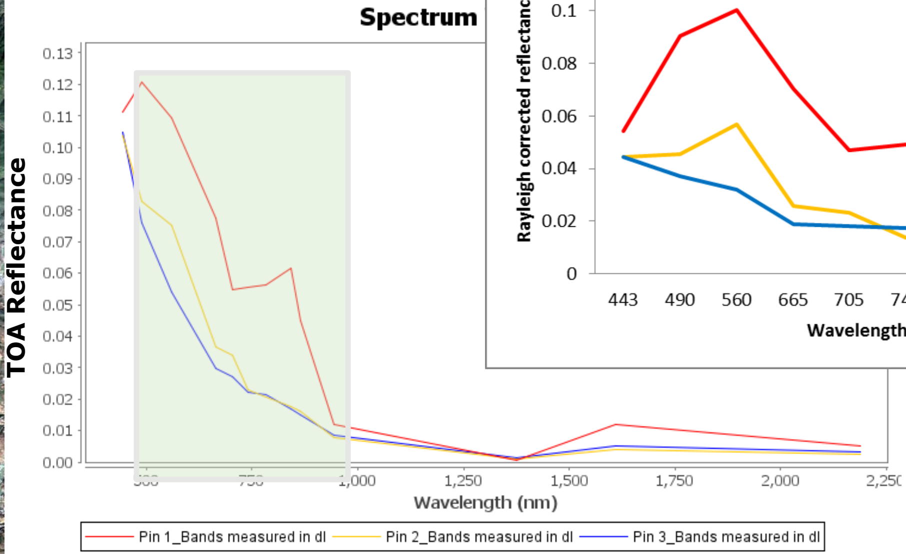

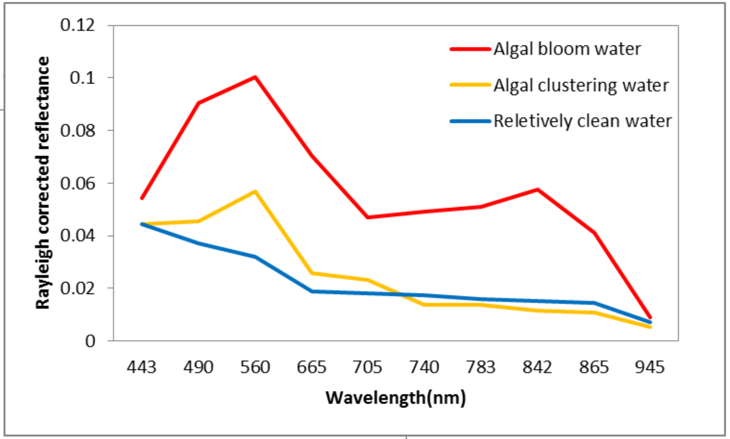

VB-FAH

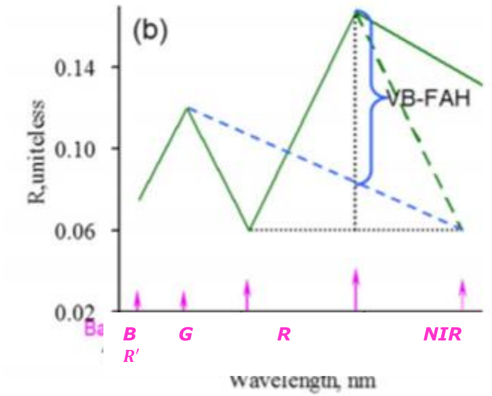

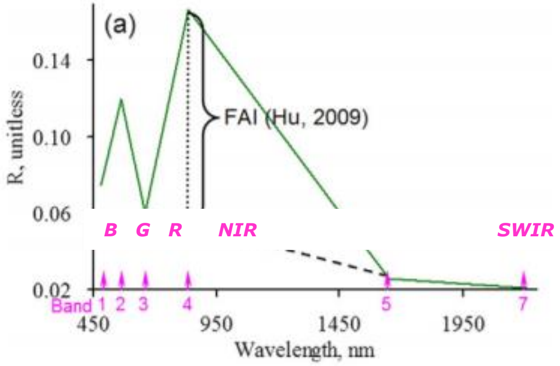

Red′ is a mirror band of Red symmetric to NIR

$$VB - FAH = R_{rc}(NIR) - R_{rc}(GREEN) + \left(R_{rc,}(GREEN) - R_{rc}(RED)\right) \times \frac{NIR - GREEN}{2 \times NIR - RED - GREEN}$$

$$FAI = R_{rc}(NIR) - R_{rc}(RED) + \left(R_{rc,}(RED) - R_{rc}(SWIR)\right) \times \frac{NIR - RED}{SWIR - RED}$$

Xing Q., Hu C. 2016, Mapping macroalgal blooms in the Yellow Sea and East China Sea using HJ-1 and Landsat data: Application of a virtual baseline reflectance height technique, Remote sensing and environment

VB-FAH calculated from MSI and OLCI

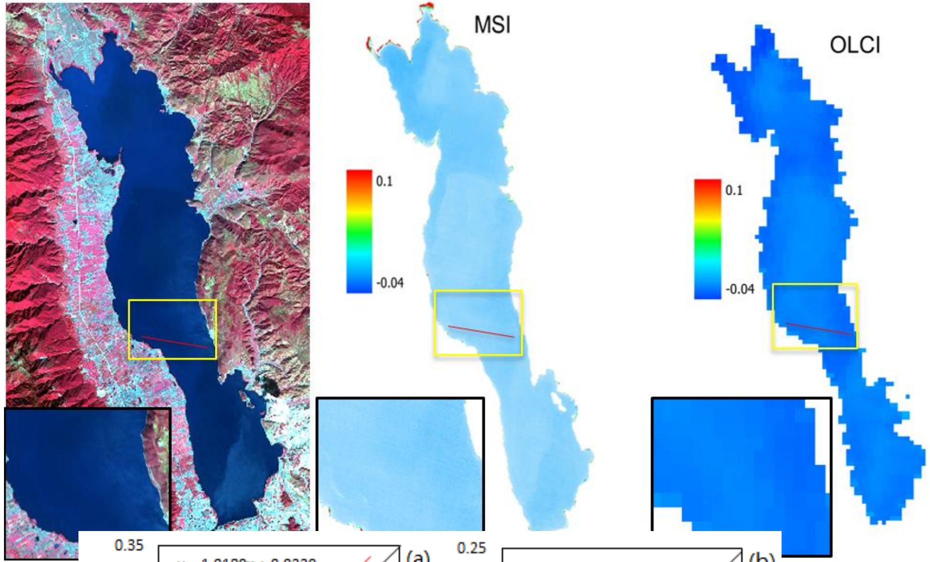

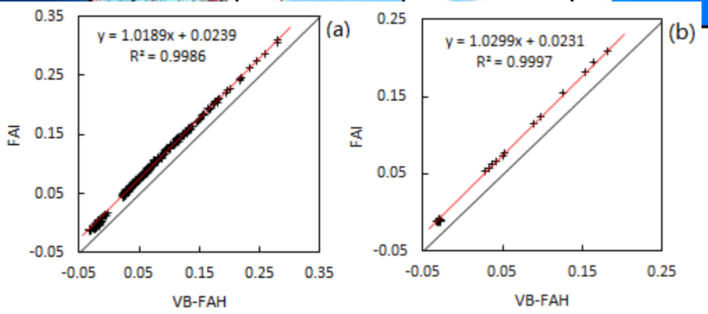

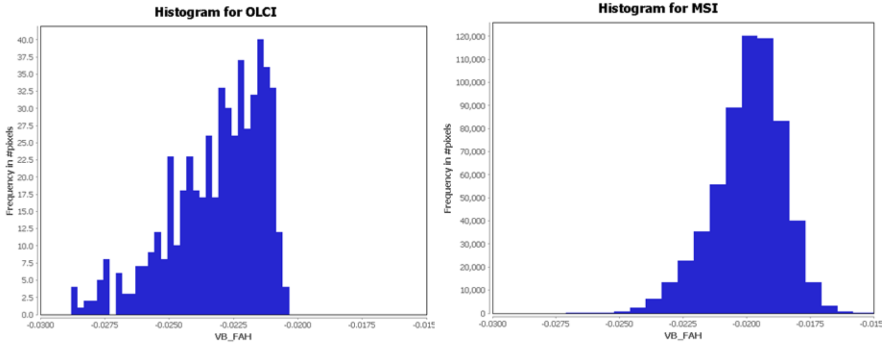

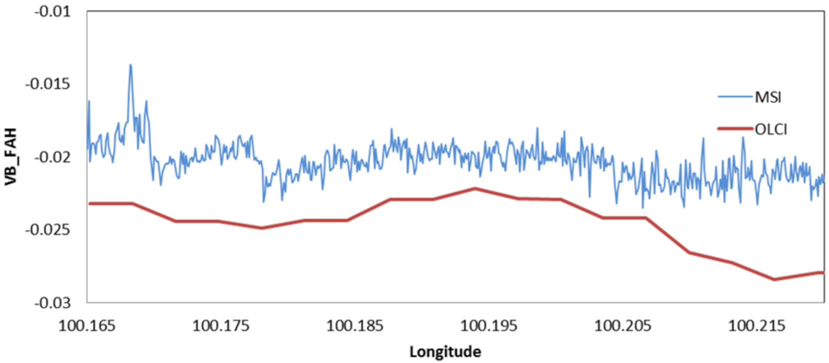

Thank you